

# Reviews

---

## Multivalent Cationic Conduction in Crystalline Solids

Joachim Köhler, Nobuhito Imanaka, and Gin-ya Adachi\*

*Department of Applied Chemistry, Faculty of Engineering, Osaka University, 2-1 Yamadaoka, Suita, Osaka 565-0871, Japan*

*Received July 7, 1998. Revised Manuscript Received August 31, 1998*

The issue “Do trivalent cations conduct in crystalline solids or not?” appears in the basic research of solid-state chemistry and deals with the characteristics and properties of a multivalent cationic current transport through a solid material. Cations in an oxidation state higher than two are not unanimously accepted as mobile species. Due to the high charge density and the resulting strong Coulombic interactions with the rigid anionic host lattice, they are expected to be rather fixed within their crystallographic sites and thus not available for the current transport. Nevertheless, some compounds are already mentioned in the literature to conduct multivalent cations. But it appears that the comprehensive demonstration and the direct verification of this phenomenon is a demanding challenge which is not completed for many of these reported multivalent conductors. On the other hand, observations and experimental data are available which unambiguously identify cations in a trivalent oxidation state as mobile charge carrying species. Such a doubtless and reliable demonstration of the migrating species in an electrochemical potential gradient can be achieved, for example, by a mutual connection of dc electrolysis experiments, electromotive force, and polarization measurements. After a careful evaluation of the literature data, it turns out that the above-mentioned question concerning the possibility of mobile multivalent cationic charge carriers in solid materials must be answered in the affirmative, even in the case of trivalent cations.

### 1. Introduction

Electrical conduction is observed when charged particles are transported by a long range migration in an electrical field gradient. The charge carriers can be either electronic (electrons or holes) or ionic (cationic or anionic) species. In contradiction to electronic conduction as in metals or semiconductors, ionic conduction is always connected with a mass transport owing to the migration of mobile ions. The phenomenon of ionic conduction can be observed in three groups of materials: liquid electrolytes, molten salts, and solid-state electrolytes. With respect to the mobile species, ionic conducting materials are commonly subdivided into the categories cationic and anionic conductors and furthermore into monovalent or multivalent conducting materials.

The principles of ionic conduction have been investigated for 100 years, and divalent ionic conduction is well-known in anionic (e.g.  $O^{2-}$  anion conductors) as well as cationic (as shown below) conductors. However, trivalent or higher valent ionic conducting materials still represent exotic compounds within the field of solidstate ionics. Cations in a high oxidation state are regarded as extremely poor mobile species due to the strong electrostatic interactions with the surrounding anionic host lattice. The topic of trivalent cationic conduction is still a controversially and emotionally discussed

subject.<sup>1</sup> Compounds which have been claimed as trivalent conductors have to be characterized by a thorough and comprehensive investigation to resist the critical comments, which brings into question the mobility of trivalent cations. As an example, the electrical properties of a 99.9% trivalent cation exchanged material are measured by impedance spectroscopy. The ionic conductivity of this ion exchanged compound decreases by more than 3 orders of magnitude and is interpreted in terms of a trivalent cationic migration. However, if the sodium concentration in the exchanged samples still remains at about 0.1% of its initial content, an exclusive current transport only by the residual  $Na^+$  cations would also possibly account for the observed conductivity after the ion exchange. Thus, the reliable and direct identification of the mobile charge carrier requires further information. Besides a various number of distinct techniques for a detailed electrical characterization, an appropriate method to directly demonstrate the migration ability of a specific ionic charge carrier is given by the Tubandt electrolysis, in which the microscopic ionic motion is unambiguously identified by corresponding macroscopic weight changes.<sup>2</sup>

From a fundamental point of view, the ion transport in solid materials is not only restricted to mobile monovalent or divalent cations but must also include higher valent species. In comparison to the huge number of mono-

valent conducting materials, only a few compounds are reported in the literature to transport multivalent cations. The purpose of this paper is (i) to give an overview of these multivalent cationic conducting compounds, (ii) to critically summarize the experimental data from which the corresponding current transport mechanism has been deduced, and (iii) to give suggestions on how the migration of mobile multivalent cations can be reliably identified. Only crystalline inorganic solid compounds have been reviewed and categorized in two groups according to the charge of mobile di- and trivalent cations.

## 2. General Considerations

Usually, ionic migration is negligible in most crystalline materials at lower temperatures, i.e., at normalized temperatures ( $T_n$ ) below 0.5 ( $T_n = T_{\text{exp}}/T_m$ , with the temperature during the measurement being  $T_{\text{exp}}$  and the melting point of the compound being  $T_m$ ). The atoms or ions are bonded tightly within their crystallographic lattice sites, and ionic movements are mainly limited to thermal vibrations. Furthermore, the migration of an ion requires crystal defects (e.g., Schottky or Frenkel defects) in the direct vicinity of the crystallographic site where the considered ion resides. These defects are usually low in concentration for most of the solid-state materials at low temperatures ( $T_n < 0.5$ ). Only at elevated temperatures, the so-called intrinsic conductivity remarkably increases due to higher thermally induced defect concentrations and the raised thermal activation for the ions.

Generally, ion transport in solid electrolytes depends on microscopic properties concerning structural features and interactions of the charge carriers with the surrounding lattice and on macroscopic properties related to thermodynamic data. In a special group of compounds, the so-called solid-state electrolytes, ions are able to move more easily. These fast ionic conducting compounds correspond at least partly to the following characteristic criteria which are necessary to facilitate ionic migration in solids.<sup>3,4</sup>

(1) A large number of mobile charge carriers must be available to sustain a reasonable current.

(2) The number of present vacant sites of identical or slightly different potential energies should be in a reasonable ratio to the number of the mobile species (tuning is possible by doping with aliovalent ions).

(3) The energy difference of the cation–anion interactions in the various sites which are involved in the conduction pathways should be small, combined with a low activation energy barrier for jumping between neighboring positions.

(4) The structure should consist of a stable framework, containing open tunnels or planes through which the mobile cations can move. The voids at the vacant sites in these opened structures are quite large, with radii greater than the minimum radii required for passing the bottlenecks between adjacent positions.

(5) Both the mobile species and the surrounding lattice atoms should be polarizable. The size of the mobile ion must be a compromise. It should be small to reduce the steric hindrance, but not too small due to enhanced interactions with the anionic lattice.

**Table 1. Comparison of the Electrical Conductivity ( $\sigma$ ) for Various Kinds of Electrolytes at Room Temperature<sup>a</sup>**

compound	$\sigma_{30^\circ\text{C}}$ [ $\Omega^{-1} \text{cm}^{-1}$ ]	
copper	$6 \cdot 10^5$	metal
concentrated $\text{H}_2\text{SO}_4$	1	liquid electrolyte
$\text{M}^+\text{Zr}_2(\text{PO}_4)_3$	$10^{-1} - 10^{-3}$	solid electrolyte
$\text{M}^{2+}\text{Zr}_4(\text{PO}_4)_6$	$10^{-3} - 10^{-8}$	solid electrolyte
NaCl	$1 \cdot 10^{-17}$	insulator

<sup>a</sup> The conductivity data of the  $\text{M}^{n+}(\text{Zr}_2(\text{PO}_4)_3)_n$  compounds correspond to the temperatures of 800–900 °C.<sup>5</sup>

(6) It is often observed that ion mobility requires low coordination numbers for the mobile ions.

For multivalent conductors, the same conditions must be met in principle to allow ionic migration. But in comparison to monovalent conducting compounds, the critical point for highly charged cations is to overcome a higher potential barrier for leaving the crystallographic sites which is caused by the stronger attraction forces to the anionic framework (conditions 3 and 5).

These electrostatic interactions can be reduced as much as possible in structures consisting of covalent frameworks which are intersected with open tunnels or layers in which spacious crystallographic sites and adequately sized bottlenecks are distributed along the migration pathways. Furthermore, the bonding energy between the mobile ions and the host lattice is weakened by competitive bonding of the anions to framework cations of high valency in ternary or quaternary compounds (e.g. tungstates, molybdates, phosphates, silicates). Indeed, all multivalent conducting compounds discussed below which exhibit reasonable conductivities at comparatively low temperatures are at least ternary compounds in non-close-packed crystal structures. But as expected, the conductivity diminishes rapidly with increasing charge of the mobile species. This behavior is due to a raised migration energy and can be rationalized from an increased lattice energy  $U$ . For example, in the Born–Mayer equation  $U$  is expressed as<sup>4</sup>

$$U = \frac{\alpha e^2 (n_+ + n_-) Z_{i+} Z_{j-}}{r} \left( 1 - \frac{\rho}{r} \right) \quad (1)$$

where  $n$  is the number and ( $eZ$ ) the charge of the cationic (+) and anionic (–) species  $i$  and  $j$  ( $e = 1.602 \cdot 10^{-19}$  C), respectively,  $\rho$  is a constant,  $r$  denotes the internuclear separation, and  $\alpha$  represents the Madelung constant of the crystal structure. The lattice energy and thus the interatomic interactions increases with the charge ( $Z_{i+}$ ), indicating a decreased mobility of the mobile ionic species which have to overcome a higher activation potential for moving through the host lattice. Table 1 shows this correlation by listing typical conductivity data of mono- and divalent cation containing  $\text{M}^{n+}(\text{Zr}_2(\text{PO}_4)_3)_n$  compounds which crystallize in the NASICON-type crystal structure. Corresponding values of an insulator, an electronic conductor, and a liquid electrolyte are added for comparison. As a general trend in  $\text{M}^{n+}(\text{Zr}_2(\text{PO}_4)_3)_n$ , when increasing the charge of the mobile species by one unit, the average ionic conductivity decreases by 2–3 orders of magnitude at temperatures about 800–900 °C. Furthermore, the higher charge density of the divalent cations and thus the increased Coulombic interactions to the anionic host

lattice are expressed by a raised activation energy for the conduction process (1.5–5.2 eV, in comparison to 0.4–0.9 eV in monovalent zirconium phosphates).<sup>5</sup>

### 3. Experimental Methods

Since the electrical conductivity of solid compounds depends on the kind and number of the charge carriers, special care has to be taken to identify the current-transporting species. In principle, the characterization of the electrical properties of a certain material consists of two main steps. First, the total electrical conductivity has to be divided into electronic (electrons or holes as charge carrier) and ionic (cations and anions as charge carrier) conductivity contributions. Second, if the compound appears to be a pure or predominant ionic conductor, the distinction between cationic or anionic conduction follows, including the identification of the corresponding charge carrier. In the case of mixed electronic/ionic conduction, the corresponding partial contributions of the single charge carriers to the total conductivity have to be determined as well. Typical mixed conductors (e.g.  $\text{Cu}_2\text{S}$ ) exhibit both high ionic and high electronic conductivity. Many compounds already have been referred to as mixed conductors if they possess only to some extent either ionic or electronic conduction. A general form of the electrical conduction theory, as developed by Wagner,<sup>6</sup> is based on the assumption that every ionic crystal is a mixed conductor. This concept should always be kept in mind when discussing a compound as an ionic conductor. If the electronic conductivity is found to be lowered by 2 orders of magnitude in comparison to the ionic conduction (electronic transference number  $< 0.01$ ), the corresponding compound is usually referred to as a pure ionic conducting material. Several experimental methods have been developed for the purpose of characterizing electrolyte materials. Here, some commonly used techniques are briefly mentioned, because they concern the subject of this review. More detailed information can be found in textbooks on electrochemistry.<sup>7,8</sup>

**Impedance Spectroscopy.** Since its first application to a solid compound in 1969 by Bauerle,<sup>9</sup> impedance spectroscopy developed into a valuable and frequently used experimental method to characterize and determine the electrical properties of ionic conductors. Detailed theoretical and practical information about impedance spectroscopy can be found in numerous publications and textbooks and will not be repeated.<sup>10,11</sup>

One of the most striking advantages of this method is the investigation of the electrical behavior of a sample without its destruction due to the application of an alternating current with a small amplitude. Even complex electrical conduction processes occurring at grain boundaries or at electrode interfaces are accessible by impedance spectroscopy. However, as a main disadvantage, the interpretation of the measured data is often difficult and ambiguous. The sample and the electrode arrangements are microscopic "black boxes" whose behavior can be interpreted with various different theoretical models. Furthermore, it is impossible to determine the nature of the charge carriers in detail. Electrical conduction, as measured by impedance spectroscopy, always represents the total conductivity of the sample, i.e., the sum of the contributions of all charge-

carrying species. But to decide whether the mobile species is of electronic, anionic, cationic, monovalent, or multivalent origin is difficult or even impossible. This question requires additional information which has to be extracted from other chemical or physical experiments. Concerning the topic of this paper, the characterization of a compound as a multivalent cationic conducting solid electrolyte only by means of impedance spectroscopical data is not sufficient. Nevertheless, impedance spectroscopy gives first insights into the electrical properties of a given system and offers some indications of the multivalent conduction phenomena. But for a more detailed characterization, further experimental methods have to be considered.

**Polarization Methods.** Polarization measurements are used to distinguish between ionic and electronic conduction and to estimate the corresponding transference number. Several modifications are possible for the experimental setup. Either a constant current (and detecting the corresponding voltage over the sample) or a constant voltage (and measuring the resulting direct current through the sample) can be applied. The voltage has to be chosen to be lower than the corresponding decomposition potential of the sample, and at least one of the two electrodes (in a two-probe setup) must be irreversible in order to block the ionic current.

In the polarization method, as originally proposed by Wagner, one ion-blocking electrode (e.g. as anode in the case of a cationic conducting electrolyte) is used while generating a low voltage.<sup>12</sup> Assuming a cation conducting sample, the charge carriers move to the cathode when applying the potential difference. Since the irreversible anode cannot supply cations for a continuous current transport, a chemical concentration gradient between the electrodes is raised. The cations are exposed to two driving forces (electrical field and concentration gradient) which act in opposite directions. Under steady-state conditions the electrical field gradient is balanced by the concentration gradient and the cationic current transport tends macroscopically to zero. In that case, the electrical conduction through the sample only depends on the migration of electronic charge carrier. From the resulting current, the dc electronic conductivity and the electronic transference number can be calculated.

In modified polarization experiments, the time dependence of the polarization behavior of a sample is determined. For example, the application of a small direct current to an ion conducting sample that is sandwiched between two ion-blocking electrodes leads to the formation of a potential difference over the sample. The ionic charge carriers migrate toward the corresponding nonreversible electrode, causing a polarization of the bulk. Within a given time, the polarization and thus the measured voltage increases and finally reaches a steady state where, microscopically, the movement of the charge carrier is balanced between chemical and electrical driving forces. For the case of partial or exclusive electronic conduction, the polarization behavior is less pronounced or not at all observable, due to the continuous supply of electrons by the electrode. Thus, the observed dc conduction is only caused by the migration of electronic charge carriers. In contrast, ac conductivity data measured by impedance

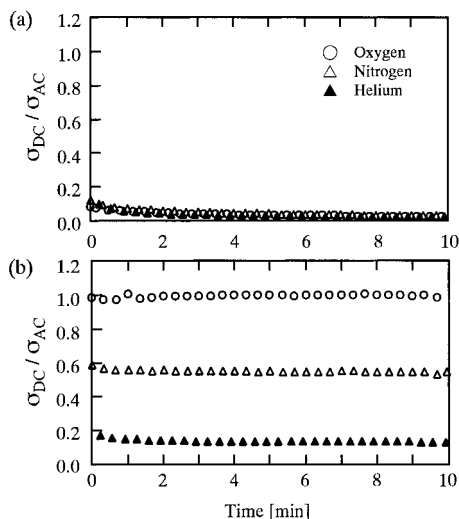


**Figure 1.** Time dependencies of the ratio  $\sigma_{dc}/\sigma_{ac}$  in atmospheres of oxygen, nitrogen ( $P_{O_2} = 2 \cdot 10$  Pa), and helium ( $P_{O_2} = 4$  Pa) for (a)  $Al_2(WO_4)_3$  and (b)  $HfO_2$  (20 mol-% CaO) at 700 °C. Reprinted from ref 13. Copyright 1997 American Chemical Society.

spectroscopy are comprised of both ionic and electronic conductivity contributions. By a comparison of the ac and dc conductivity the corresponding transference number can be determined.

Furthermore, these polarization measurements are a useful tool to determine the single conductivity contributions of different ionic species which may be mobile within the material. For example, in cationic conductors based on oxygen or nitrogen containing crystal structures, the mobility of these anions has to be checked in order to relate the observed conductivity only to the migration of cations. For hygroscopic compounds, such as the  $\beta$ -Aluminas, a possible protonic motion which may be caused by the incorporation and dissociation of water molecules has also to be examined. To illustrate the method, the time dependencies of the dc and ac conductivity ( $\sigma_{dc}/\sigma_{ac}$ ) are comparatively investigated for  $Al_2(WO_4)_3$  and  $HfO_2$  (stabilized with 20 mol % CaO) in oxygen, nitrogen, and helium, respectively.<sup>13</sup> The corresponding data are plotted in Figure 1. In  $Al_2(WO_4)_3$ , which is a pure trivalent cationic conductor, the polarization behavior is similar in the different atmospheres. The dc conductivity (electronic conductivity) drops down to values below 1% of the total electrical conductivity, which is measured by impedance spectroscopy. This result indicates that the electronic contributions to the total electrical conductivity are negligible. Furthermore, the identical polarization behavior in oxygen, nitrogen ( $P_{O_2} = 2 \cdot 10$  Pa), and helium ( $P_{O_2} = 4$  Pa) atmospheres suggests a negligible influence of the oxide anions on the conduction properties. Thus,  $O^{2-}$  anions can be excluded as mobile charge carriers in  $Al_2(WO_4)_3$ . On the contrary, the  $O^{2-}$  anion conductor  $HfO_2$  (20 mol % CaO),<sup>14</sup> which exhibits a comparable electrical conductivity to  $Al_2(WO_4)_3$ , shows a clear dependence on the oxygen partial pressure. The dc conductivity is identical to the ac data which have been obtained in a pure oxygen atmosphere. With declining oxygen partial pressure, the dc conduction is lowered gradually, indicating oxygen anions as charge carriers. Thus, a clear distinction between cationic and  $O^{2-}$  anionic conduction becomes possible. Conductivity con-

tributions by nitrogen anions or protons can be investigated by measuring the dependence of conductivity on the nitrogen or hydrogen partial pressure, respectively.

**Electromotive Force Measurements.** Measurements of the electromotive force (EMF) in galvanic concentration cells represent important and powerful methods for determining transference numbers and for estimating the nature of the charge carrier in solids. An EMF appears when a solid electrolyte is fixed between two electrodes exerting different chemical potentials to the mobile ions. From the Nernst equation the theoretical EMF value can be calculated according to a defined cell reaction, which assumes a chemical reaction between the electrode material and the mobile species after its migration through the electrolyte. If this theoretical EMF corresponds with the observed experimental data, the mobile species is identified (according to the theoretical cell reaction) with a transference number of unity. However, it must be ensured that the observed EMF is originated by the exclusive migration of the considered ion. If different kinds of charge carriers are present and able to respond to the electrochemical potential difference, the measured EMF does not correspond to the theoretical cell reaction and the measurement becomes meaningless. For example, in cationic conducting compounds with an oxide-based host lattice the current transport by oxygen anions might be possible when using electrodes which operate with different oxygen partial pressures. This possibility must be investigated in additional experiments and excluded in order to unambiguously interpret the EMF data within the considered experimental setup. If it is possible to attribute the observed EMF to only one charge carrier (the multivalent cation), this method strongly indicates the mobility of the considered ion. Even in combination with the aforementioned polarization and impedance spectroscopic measurements, a nearly completed electrical characterization of the ion conducting material becomes possible. When performing additional dc electrolysis experiments, a direct and finally comprehensive demonstration about the nature and charge of the mobile charge carriers can be realized.

**Electrolysis Experiments.** The electrolysis of a solid electrolyte material appears to be a valuable method to provide direct evidence for the migration of a specific mobile ionic species. It is possible to observe and to quantitatively measure the macroscopic transport of ions through a solid electrolyte. The techniques discussed so far only give indirect evidence by connecting theoretical models with experimental data. On the other hand, electrolysis experiments offer the possibility to directly detect the migrating species and to make definite statements about its nature, such as charge or oxidation state. The results of electrolysis experiments are most important for the characterization of an ionic conducting material in comparison to other electrochemical methods.

Several experimental setups are available to perform electrolysis experiments. The simplest one is to apply a voltage higher than the corresponding decomposition potential for a given time to a bulk sample and to characterize the cathodic and anodic surfaces of the material before and after the electrolysis. Considering a cationic conducting material, the migration of the

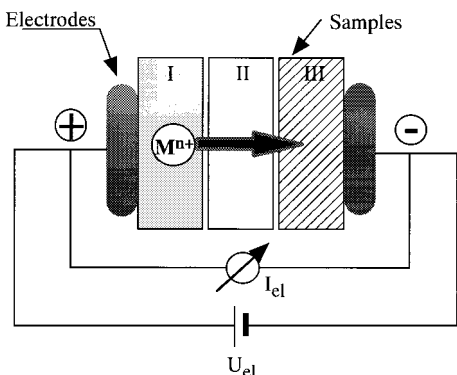


**Figure 2.** Schematic view for a dc electrolysis experiment using the Tubandt method. Applying a voltage  $U_{el}$  leads to a measurable current  $I_{el}$  which is transported by the migration of cations ( $M^{n+}$ ) toward the cathode.

mobile cations toward the cathode occurs during the procedure. Thus, the cation/anion ratio at the cathodic (anodic) side of the pellet should be relatively increased (decreased), in comparison to the value before the electrolysis. However, just detecting such an increased cation concentration on the cathodic surface is not a sufficient criterion to ensure the migration process of this cation through the solid. Similar results can also be obtained by a simple decomposition of the sample and adhering material to the cathodic electrode, which lead to falsified intensity ratios of the remaining sample. To exclude those experimental errors, additional chemical analysis has to be done for the electrode surfaces as well as for the bulk. For example, by monitoring the cross-section line between the anode and cathode of the electrolyzed sample by EPMA (electron probe microanalysis), the exact concentration profile of the considered ion can be obtained. In the case of cationic conduction, the cation concentration at the cathodic surface should be increased in comparison to the bulk concentration, indicating the mobile nature of the regarded species with its accumulation on the cathodic side. Furthermore, after the migration through the solid bulk, the mobile cations chemically react at the cathodic surface with the remaining solid, the atmospheric gases, or the cathodic material (most often the corresponding oxides of the mobile cations are formed when performing the experiments in air atmosphere). For an exact characterization of the cationic migration process, it is necessary to analyze these products, which ideally form single deposits on the surface of the electrolyte. The combination of these analytical procedures, especially the measurement of a concentration profile within the bulk and a chemical analysis of surfaces and deposits, reliably verifies the ion transport through the solid.

Sophisticated dc-electrolysis techniques, e.g. the Tubandt method, do not only use one but two or three bulk samples for which the decomposition voltage is simultaneously applied. The ionic motion can be directly evidenced by corresponding weight changes in the single bulk phases. The original experimental setup of the Tubandt electrolysis was introduced in 1932 by Tubandt and co-workers.<sup>2</sup> A constant current is passed through three separate pellets of the sample which are sandwiched between two electrodes, as is shown schematically in Figure 2. If the electrical transport through the sample is of ionic origin, characteristic weight changes

occur in the anionic and cationic parts of the system. For the case of cationic conduction and the use of two ion-blocking electrodes, the anodic pellet decreases, the cathodic one increases, and the centered sample ideally remains constant in weight. From the current which passed through the sample, the valency and the transference number can be determined according to Faraday's law. As the weight changes in the pellets agree with Faraday's law, the current transport must be purely ionic with an electronic transference number of zero. Such electrolysis experiments finally provide the qualitative as well as quantitative demonstration of the nature of the charge carrier, its valency, and its transference number. Misinterpretation is only possible, if more than one mobile species are present within the sample. To elucidate the fundamental question concerning mobile multivalent ( $n > 2$ ) cations in solids, the Tubandt-electrolysis experiment is an imperative method.

#### 4. Multivalent Cationic Conduction

In the subsequent sections, compounds for which a multivalent cationic conduction is reported will be presented. Emphasis is given to the experimental data which have been used to derive the assumptions for the corresponding ion transport. It appears that for some compounds a multivalent cationic conduction has been concluded without a completed and unambiguous characterization. Multivalent cationic conduction might occur within these materials, but from a critical point of view some doubts remain which should be eliminated by additional investigations.

The extraordinary high ionic conductivity of solid silver iodide was discovered in 1921 by Tubandt and co-workers.<sup>15,16</sup> This observation initiated intense research which resulted in the discovery and creation of a huge number of compounds exhibiting ion conduction characteristics. As for cationic conducting materials, most of these compounds transport monovalent cations (e.g.,  $Li^+$ ,  $Na^+$ ), whereas multivalent cationic conductors are only rarely mentioned. Reports on the migration of multivalent cations based on thermally induced diffusion processes date back to the beginnings of solid-state ionics research. Divalent cation migration in a solid material was first observed for  $PbCl_2$  and  $PbI_2$ , which were thus far known as anion conductors only. But by doping with aliovalent compounds, like  $LaCl_3$  or  $ThCl_4$ ,  $Pb^{2+}$  vacancies are generated and the  $Pb^{2+}$  cations become able to diffuse at small but measurable rates. The transference number was quantitatively determined from electrolysis experiments and amount to  $t_{Pb^{2+}} = 0.1-0.2$  for the  $Pb^{2+}$  cations ( $t_{Cl^-} = 0.8-0.9$  for the  $Cl^-$  anions) at 280 °C.<sup>17</sup> But despite the partial  $Pb^{2+}$  mobility, these compounds are usually not regarded as divalent cationic conducting electrolytes, due to the major current transport by anions.

Another kind of di- and trivalent cationic motion is given for the diffusion of  $^{109}Cd^{2+}$  and  $^{111}In^{3+}$  tracer isotopes within the superionic phases  $\alpha-Ag_2S$ ,  $\alpha-Ag_2Se$ , or  $\alpha-Ag_3SI$ , which crystallize in the  $\alpha-AgI$ -type structure.<sup>18</sup> Comparable high mobilities and low activation energies for the diffusive multivalent cationic transport have been observed. But due to the low concentration of multivalent impurities (less than 10 ppm) and the resulting nearly exclusive current transport by the

highly mobile monovalent  $\text{Ag}^+$  ions, these compounds are still treated as monovalent solid electrolytes. However, these measurements already demonstrate the basic concept of how to create new electrolyte materials by using the crystal structure of known fast ionic conducting compounds as a host lattice for multivalent cations. Many of the present multivalent conducting compounds are based on this idea, as will be shown in the next sections for materials which have been derived from, for example, the fast ion conducting  $\beta$ -Aluminas or NASICON electrolytes.

A further interesting example, even with regard to a multivalent cationic diffusion process, is given by solid solution compounds in the  $\beta$ - $\text{Si}_3\text{N}_4$ - $\text{Al}_2\text{O}_3$  system (so-called  $\beta$ -sialons). At temperatures above 1000 °C, the  $\beta$ -sialons generate conductivities of about  $10^{-4}$ – $10^{-6} \Omega^{-1} \text{cm}^{-1}$ , which are assumed to be due to a tetravalent  $\text{Si}^{4+}$  transport.<sup>19</sup> This conclusion has been extracted from an electrolysis experiment in which an increased Si concentration at the cathodic surface of the electrolyzed samples was detected by EPMA and interpreted to result from a  $\text{Si}^{4+}$  migration through the sample. But there are no reports on the determination of electronic and ionic transference numbers for this compound. Neither the cross-sectional concentration profile nor an analysis of the compounds on both sample surfaces was given. It cannot certainly be excluded that the observed results may have been caused by decomposition reactions at the electrodes or by a transport of nitrogen anions. However, if the  $\text{Si}^{4+}$  migration can be unambiguously identified in additional experiments, these  $\beta$ -sialon compounds become the first tetravalent cationic conductors which would open a new field of fundamental research in solid-state ionics.

The first systematic investigations on a divalent solid electrolyte have been performed on CaS, since it was found to conduct  $\text{Ca}^{2+}$  cations.<sup>20</sup> Although the conductivity is rather low (only  $10^{-6}$ – $10^{-8} \Omega^{-1} \text{cm}^{-1}$  at 770 °C),<sup>20–25</sup> a macroscopic  $\text{Ca}^{2+}$  transport could be directly demonstrated in modified Tubandt-electrolysis experiments, determining the transference number of the mobile cation to be nearly unity ( $t_{\text{Ca}^{2+}} > 0.95$ ).<sup>21</sup> CaS is the first solid electrolyte material for which a predominant divalent cationic migration could be qualitatively and quantitatively demonstrated.

With the synthesis of divalent  $\text{M}^{2+}$ - $\beta$ - $\text{Al}_2\text{O}_3$  or  $\text{M}^{2+}$ - $\beta''$ - $\text{Al}_2\text{O}_3$  compounds in 1967 ( $\text{M}^{2+}$ - $\beta$ - $\text{Al}_2\text{O}_3$ )<sup>26</sup> and 1980 ( $\text{M}^{2+}$ - $\beta''$ - $\text{Al}_2\text{O}_3$ )<sup>27,28</sup> by ion exchange reactions from the corresponding  $\text{Na}^+$ - $\beta$ - and  $\beta''$ -aluminas, a new group of divalent cationic conductors became available, exhibiting higher conductivities at reasonable temperatures (reports of divalent ion exchange reactions on  $\text{Na}^+$ - $\beta$ - $\text{Al}_2\text{O}_3$  already existed since 1940, but no electrical measurements were reported).<sup>29</sup> Trivalent cationic conduction is also reported to occur since the successful incorporation of trivalent lanthanide ions (Ln) into the layered structure of  $\text{Na}^+$ - $\beta''$ - $\text{Al}_2\text{O}_3$  in 1983.<sup>30</sup> The  $\text{Ln}^{3+}$ - $\beta''$ - $\text{Al}_2\text{O}_3$  have been mentioned as trivalent solid electrolytes exhibiting comparatively high conductivities ( $\sigma_{500^\circ\text{C}} = 10^{-5}$ – $10^{-6} \Omega^{-1} \text{cm}^{-1}$ ). The multivalent cationic migration properties in the  $\beta$ -alumina host lattice are demonstrated by the possibility of ion exchange reactions. Nearly the entire  $\text{Na}^+$  content can be replaced during the exchange procedure, where the multivalent

cations migrate macroscopic distances within the samples. In divalent  $\text{M}^{2+}$ - $\beta''$ -aluminas, various electrical measurements have been used to characterize the conduction properties in further detail. Little doubt remains for these materials concerning the divalent migration abilities. Since trivalent  $\text{M}^{3+}$ - $\beta$ -aluminas are also prepared by ion exchange reactions, a trivalent cationic mobility within the conduction layers can be assumed in analogy. Thus, the  $\text{M}^{3+}$ - $\beta$ -aluminas are already widely accepted trivalent cationic conductors. However, it should be mentioned that although the phenomenon of trivalent cationic mobility has been supported by conductivity as well as X-ray diffraction measurements, no direct evidence for the migration of the trivalent charge carrier in an electric gradient has been presented so far. Results of corresponding experiments would complete the research about fundamental trivalent cationic migration properties within these compounds.

Recently, another group of materials, compounds in the  $\text{Sc}_2(\text{WO}_4)_3$ -type structure, gained interest with respect to an unambiguous identification of a trivalent cationic current transport. For example, in electrolysis, electromotive force, as well as polarization measurements,  $\text{Al}^{3+}$  cations could be qualitatively and quantitatively determined to be the conducting species in  $\text{Al}_2(\text{WO}_4)_3$ , generating an  $\text{Al}^{3+}$  cationic conductivity of  $\sigma_{800^\circ\text{C}} = 2 \cdot 10^{-5} \Omega^{-1} \text{cm}^{-1}$ .<sup>13</sup>

## 5. Divalent Cationic Conductors

**5.1. CaS Type Phases.** It seems to be surprising that in this paper the electrical properties are described for a compound that crystallizes in the close-packed NaCl-type structure. Indeed, pure calcium sulfide exhibits only poor conductivity due to lacking opened regions such as tunnels or layers in the crystal structure as well as a sufficient number of vacant sites for the conduction process. Only at high temperatures does the defect concentration within the crystal lattice increase, resulting in reasonable conductivities ( $\sigma_{770^\circ\text{C}} = 10^{-6}$ – $10^{-8} \Omega^{-1} \text{cm}^{-1}$ ).<sup>20–25</sup> However, interest in this compound arose since it was recognized that this conductivity is caused by  $\text{Ca}^{2+}$  cationic conduction and since application as a solid electrolyte for the determination of sulfur chemical potentials became possible. By homogeneous doping with aliovalent cations, e.g.  $\text{La}_2\text{S}_3$  or  $\text{ZrS}_2$ , the electrical properties can be remarkably improved due to the creation of  $\text{Ca}^{2+}$  vacancies.<sup>22</sup> As a disadvantage, the electrical conductivity depends on the sulfur partial pressure ( $P_{\text{S}_2}$ ), and increased electronic conductivities are observed at lower as well as at higher sulfur pressures. A predominant  $\text{Ca}^{2+}$  conduction has been reported for undoped CaS for  $P_{\text{S}_2} < 10^{-5}$  atm. The transference number ( $t_{\text{Ca}^{2+}}$ ) for the  $\text{Ca}^{2+}$  migration in this  $P_{\text{S}_2}$  region was directly determined from modified Tubandt electrolysis experiments to be nearly unity ( $t_{\text{Ca}^{2+}} > 0.95$ ).<sup>21</sup> Thus, it can be stated that CaS is the first solid electrolyte for which a predominant divalent cationic conduction has been qualitatively and quantitatively identified.

Doping effects, similar to those in CaS, are observed in the isotype crystallizing compound  $\text{SrS}$ .<sup>31,32</sup> The electrical conductivity could also be improved by the formation of solid solutions with aliovalent rare earth sulfides. But in comparison to the CaS phases, the

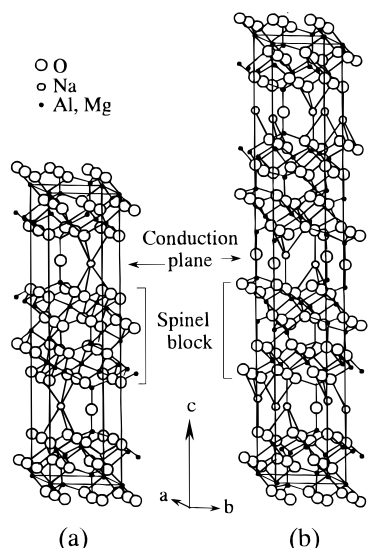


**Figure 3.** Idealized representation of the crystal structures of (a)  $\text{Na}^+\text{-}\beta\text{-Al}_2\text{O}_3$ ,  $a \approx 5.6 \text{ \AA}$ ,  $c \approx 22.5 \text{ \AA}$  ( $P6_3/mmc$ ),<sup>33</sup> and (b)  $\text{Na}^+\text{-}\beta''\text{-Al}_2\text{O}_3$ ,  $a \approx 5.6 \text{ \AA}$ ,  $c \approx 33.7 \text{ \AA}$  ( $R\bar{3}m$ ).<sup>34</sup>

electrical properties of the doped SrS compounds are not thoroughly characterized, and a detailed determination of the charge carriers is not available at the moment. However, due to similar observations in the conduction behaviors between SrS and CaS, a current transport by divalent cations ( $\text{Sr}^{2+}$ ) is also assumed to occur in doped SrS.

**5.2.  $\beta$ -Alumina (General Remarks).** There exists a large number of compounds belonging to the family of  $\beta$ -Alumina ( $\beta$ -aluminum oxides) exhibiting similar crystal structures but different compositions. Some of these compounds have become important materials for the research in solid electrolytes. Due to the unusual crystal structure as well as the ionic conducting properties, generating high ionic and low electronic conductivity, these compounds are not only of interest for the development of technical applications (e.g. Na/S batteries) but also for the purpose of acting as a source for various kinds of new solid electrolytes, including multivalent cation conducting compounds.

The most important and well-known compounds in this family are  $\text{Na}^+\text{-}\beta\text{-alumina}$  ( $\text{Na}^+\text{-}\beta\text{-Al}_2\text{O}_3$ ) and  $\text{Na}^+\text{-}\beta''\text{-alumina}$  ( $\text{Na}^+\text{-}\beta''\text{-Al}_2\text{O}_3$ ).  $\text{Na}^+\text{-}\beta\text{-Al}_2\text{O}_3$ , for which the ion conducting properties were discovered in 1969,<sup>26</sup> crystallizes in the nonstoichiometric composition  $\text{Na}_{1+x}\text{Al}_{11}\text{O}_{17+x/2}$  ( $0.2 \leq x \leq 0.7$ ) with an excess amount of sodium.  $\text{Na}^+\text{-}\beta''\text{-Al}_2\text{O}_3$ , a metastable structural modification of  $\text{Na}^+\text{-}\beta\text{-Al}_2\text{O}_3$ , requires mono- or divalent oxides (like  $\text{Li}_2\text{O}$  or  $\text{MgO}$ ) for its stabilization to give the ternary oxide with a nonstoichiometric composition  $\text{Na}_{1+x}\text{Mg}_x\text{Al}_{11-x}\text{O}_{17}$  ( $0.3 \leq x \leq 0.8$ ) for the case of MgO stabilization.

**Crystal Structure.** The crystal structures of  $\text{Na}^+\text{-}\beta\text{-Al}_2\text{O}_3$  and  $\text{Na}^+\text{-}\beta''\text{-Al}_2\text{O}_3$  consist of the same building principle as shown in Figure 3. Both compounds crystallize in a layered structure which can be described in terms of alternating sequences (in the  $c$ -direction) of close-packed  $\text{Al}_{11}\text{O}_{16}$  or  $\text{MgAl}_{10}\text{O}_{16}$  groups (so-called spinel blocks, due to the similar atomic arrangement as in the spinel structure of  $\text{MgAl}_2\text{O}_4$ ) sandwiching loosely packed NaO or  $\text{Na}_2\text{O}$  layers. Stabilizing  $\text{Mg}^{2+}$  ions in the  $\text{Na}^+\text{-}\beta''\text{-Al}_2\text{O}_3$  phase are found exclusively

within the spinel blocks. The main difference of the two alumina phases concerns the atomic arrangement within the layers. Three crystallographic nonequivalent sites are available for the sodium cations in the conduction planes of  $\text{Na}^+\text{-}\beta\text{-Al}_2\text{O}_3$  [the eight-coordinated mid-oxygen site (mO), the nine-coordinated Beavers-Ross-type position (BR), and the five-coordinated anti-Beavers-Ross-type position (aBR)], but only two are present in  $\text{Na}^+\text{-}\beta''\text{-Al}_2\text{O}_3$  [the eight-coordinated mid-oxygen site (mO) and the seven-coordinated Beavers-Ross-type position (BR)]. More detailed information on the crystal structures can be found in the literature.<sup>26,33,34</sup>

**Electrical Properties and Preparation Methods.** The lowered oxygen occupation in the inter-spinel layers causes a high  $\text{Na}^+$  cationic mobility due to (i) a high number of available sites for the migrating cations, (ii) reduced Coulombic attraction forces to the migrating cations, and (iii) an opening of the interspinel layers in comparison to the close packed spinel blocks. The anisotropic crystal structure reflects the two-dimensional nature of the ionic conduction which occurs within the opened planes (the so-called conduction planes). The ionic conductivity perpendicular and parallel to the crystallographic  $c$ -axis differs by several orders of magnitude in both compounds. For the in-plane conduction (perpendicular to the  $c$ -axis)  $\sigma$ -values of about  $10^{-2}\text{--}10^{-3} \text{ }\Omega^{-1} \text{ cm}^{-1}$  are observed at room temperature.<sup>35-37</sup> The structure stabilizing cations (e.g.  $\text{Li}^+$ ,  $\text{Mg}^{2+}$ ) in  $\text{Na}^+\text{-}\beta''\text{-Al}_2\text{O}_3$  are usually located within the spinel blocks and are not expected to contribute to the ionic conductivity, which is exclusively originated from the mobile cations within the conduction layers. But the presence of even a small amount of these cations within the conduction planes may be possible and should be considered for the interpretation of conductivity data. In comparison,  $\text{Na}^+\text{-}\beta\text{-Al}_2\text{O}_3$  does not have this problem since there are no structure-stabilizing additives necessary.

Due to the fast diffusion properties of the cations in the conduction planes, the sodium ions can be almost completely replaced by other mono-, di-, or trivalent cations in simple ion exchange reactions generating new types of solid electrolytes ( $\text{M}^{n+}\text{-}\beta\text{-Al}_2\text{O}_3$  and  $\text{M}^{n+}\text{-}\beta''\text{-Al}_2\text{O}_3$ ) containing various kinds of cations  $\text{M}^{n+}$ ,<sup>26-28,38-44</sup> which are also assumed to be mobile. But so far, this fundamental question whether and to what extent the multivalent cations are mobile is not uncontested. Although the ion exchange reactions strongly indicate the ability of the multivalent cations to migrate macroscopic distances, there are still some critics doubting these materials as multivalent conductors, especially for the case of trivalent cationic conduction. The cations enter the unexchanged crystals by diffusion in a chemical potential gradient. However, from a basic point of view, it has not been demonstrated yet that trivalent cationic diffusion is identical to the migration of trivalent cations in an electric potential gradient. It is widely accepted that both migration phenomena can be treated in the same way and even the well-known Nernst-Einstein equation quantifies this relation by connecting the diffusion coefficient with the electrical conductivity. The Nernst-Einstein equation has already been proven to be correct for monovalent cationic conducting systems and also for divalent  $\text{M}^{2+}\text{-}\beta''\text{-Al}_2\text{O}_3$  (section 5.2.3).

However, corresponding experiments in which the Nernst–Einstein equation is explicitly verified for the case of trivalent cationic conduction are not reported (i.e., measurement and comparison of the chemical and the electrical diffusion coefficient). But it is possible to calculate a diffusion coefficient from ion exchange data in  $M^{3+}\text{-}\beta''\text{-Al}_2\text{O}_3$  ( $M = \text{Pr, Gd}$ ) and to relate it to the conduction data of impedance spectroscopic measurements on the corresponding compounds (section 6.1.1). This calculation indicates the validity of the Nernst–Einstein equation also for mobile trivalent cations. But in order to obtain a more reliable evidence, the migration of a trivalent charge carrier in an electrical field should be directly demonstrated in appropriate measurements, e.g. dc electrolysis experiments.

To give an impression about the ongoing controversial discussion, some remarks concerning the possibilities and problems that arise during the preparation and characterization of multivalent  $M^{n+}\text{-}\beta$ -aluminas are described. Usually, the ion exchange is performed by the molten salt technique, i.e., immersing polycrystalline or single-crystal material of  $\text{Na}^+\text{-}\beta\text{-Al}_2\text{O}_3$  or  $\text{Na}^+\text{-}\beta''\text{-Al}_2\text{O}_3$  at elevated temperatures into a fused salt which contains the corresponding cation  $M$  (most often anhydrous nitrates or halides are used). The degree of the ion exchange can be controlled by (i) varying the composition of the salt (by forming eutectic mixtures with corresponding sodium salts), (ii) changing the temperature at which the exchange reaction takes place or (iii) controlling the exposure time of the samples to the melt. Furthermore, for a given reaction condition, the exchange properties depend on size and charge of the replacing cation as well as on the composition of the base  $\text{Na}^+\text{-}\beta$ - or  $\text{Na}^+\text{-}\beta''\text{-Al}_2\text{O}_3$  crystals.<sup>43,44</sup>

Alternatively, ion exchange reactions can be performed in the vapor phase generated by the halide or nitrate salts. In this technique, the  $\beta/\beta''$ -alumina material is covered with the corresponding salt, which is heated to below its melting point. The ion exchange proceeds by a vapor phase transport of the species entering and leaving the sample.<sup>43</sup> This method provides more gentle conditions at lower temperatures, preventing thermal degradation of the crystals. However, vapor phase exchange reactions are much slower compared with those of the molten salt technique and often produce incomplete exchanged samples.

Although ion exchange reactions, either by the molten salt or vapor phase methods, are in most cases simple to perform and straightforward, sometimes a quite complex behavior is observed. Especially cations that can exist in different oxidation states [e.g.  $\text{Cu(I)}/\text{Cu(II)}$ ,  $\text{Co(II)}/\text{Co(III)}$ ,  $\text{Eu(II)}/\text{Eu(III)}$ ] cause problems in maintaining the desired oxidation state during the exchange reaction. Most often, the tendency to reduce the incorporated cations by the simultaneous loss of oxygen can be observed. Special care has to be taken in these cases when selecting the ion exchange conditions, to ensure the desired oxidation state of the replacing cations.

Nevertheless, the ion exchange reaction provides a valuable method for preparing new materials at moderate temperatures. Even compounds which are metastable at higher temperatures and not accessible by direct synthesis, e.g. most of the multivalent phases, can be formed. However, the exchange characteristics are

quite different between  $\text{Na}^+\text{-}\beta\text{-Al}_2\text{O}_3$  and  $\text{Na}^+\text{-}\beta''\text{-Al}_2\text{O}_3$  and between single or polycrystalline material. As a general trend,  $\beta''$ -alumina compounds replace the cation content much faster than  $\beta$ -aluminas and single crystals are remarkably easier to ionically exchange than polycrystals.

Another problem of the ion exchange method is of a more fundamental nature and is most often argued by critics. Referring to statistical considerations, the ion exchange cannot be completed up to 100%. Usually, the termination of a “complete ion exchange” describes ion-exchanged samples where the  $\text{Na}^+$  concentration is reduced by at least 3 orders of magnitude. Thus,  $M^{n+}\text{-}\beta\text{-Al}_2\text{O}_3$  and  $M^{n+}\text{-}\beta''\text{-Al}_2\text{O}_3$  material, prepared by ion exchange from the corresponding  $\text{Na}^+$  compounds, always contains residual sodium ions up to 0.1% of the original  $\text{Na}^+$  content. At low temperatures ( $T \leq 100\text{--}200\text{ }^\circ\text{C}$ ), the multivalent cations are considered to be trapped within their positions and the conductivity is only transported by the residual sodium ions. At higher temperatures, the multivalent cations are assumed to become mobile, but the present  $\text{Na}^+$  migration influences the conduction characteristics and give some aspects of uncertainty to its interpretation. The conductivity in  $\text{Na}^+/\text{M}^{n+}\text{-}\beta$ - and  $\text{Na}^+/\text{M}^{n+}\text{-}\beta''\text{-Al}_2\text{O}_3$  compounds is complex in nature and influenced by many parameters, e.g., size, polarizability, and concentration of the mobile cations, distribution of the cations in the available sites, and spacing of the conduction slabs. The effect of remaining  $\text{Na}^+$  ions on these parameters is not characterized in detail yet.

As an alternative way to prepare multivalent  $M^{n+}\text{-}\beta/\beta''$ -aluminas, the direct synthesis at higher temperatures is applied in conventional solid-state reactions by directly using the corresponding multivalent cation containing compounds as starting materials (without monovalent  $\text{Na}^+$  cations). At a first glance, this method seems to be appropriate to decide whether the influence of residual sodium ions on the conductivity data in multivalent cation exchanged samples can be neglected or not. However, it should be mentioned that even the directly synthesized  $M^{n+}\text{-}\beta/\beta''$ -alumina compounds might contain sodium cations (or other cations) within the conduction planes which originate from impurities in the used starting reagents. This aspect is difficult to estimate due the lack of specifications in the corresponding literature concerning the purity of the materials. Assuming “usual” purity of 99.9–99.99% for the available reagents, the concentration of cationic impurities which are able to enter the conduction planes during the synthesis might be on the same order of magnitude in comparison to the concentration of residual  $\text{Na}^+$  cations (or other impurities) in ion-exchanged samples. For further investigations, the  $\text{Na}^+$  content of both ion-exchanged and directly synthesized  $M^{n+}\text{-}\beta/\beta''$ -alumina should be accurately determined and compared to each other for a reliable interpretation of the conductivity data in each system.

The direct synthesis technique is connected to further fundamental problems. Only polycrystalline material can be produced, and the elevated temperatures which have to be applied often cause deterioration and/or the formation of multiphased products. In particular  $\beta''$ -aluminas are metastable at high temperatures and suffer decomposition or transformation into  $\beta$ -alumina,



magnetoplumbite-type, or other phases. In comparison to the ion exchange method, only a limited number of  $M^{n+}$ - $\beta/\beta''$ -alumina compounds are accessible by direct synthesis.

A problem that concerns the electrical properties of both ion-exchanged as well as directly synthesized  $M^{n+}$ - $\beta/\beta''$ -alumina is caused by their hygroscopic behavior and the ability to incorporate water molecules into the conduction planes. These molecules dissociate and might lead to protonic conduction. In addition to the conductivity contributions of impurities or residual sodium cations, the possible protonic current transport adds a further aspect of uncertainty to the measured conductivity data that must also be taken into account for the corresponding interpretation in terms of multi-valent cationic conduction. The presence of protonic conduction can be estimated by measuring the dependence of polarization behavior and conduction properties on the hydrogen partial pressure. If the polarization behavior and the electrical conductivity of the samples remain unchanged, even in a pure hydrogen atmosphere, a protonic conduction process can be excluded.

Comparing the electrical properties of corresponding  $\beta$ - and  $\beta''$ -alumina materials, single crystals always exhibit higher conductivities than polycrystalline material and  $\beta''$ -aluminas are the better ion conductors than  $\beta$ -aluminas compounds in the same crystallization state. However, despite the decreased conduction ability, many potential applications will require rather dense polycrystalline material which is more appropriate for the fabrication of compacts in a required shape than single-crystal material. Polycrystalline  $M^{n+}$ - $\beta/\beta''$ -alumina compounds have been already widely used as electrolytes in electric cells for thermodynamic studies or for some sensor applications. Due to the higher thermal stability, polycrystalline  $\beta$ -alumina compounds are often preferred in technical devices, instead of polycrystalline  $\beta''$ -aluminas. Single crystalline material is not of great importance in electric applications. It has been used for investigations concerning fundamental research, such as the elucidation of conduction mechanisms or the investigation of conductivity dependencies on structural chemistry. Furthermore, it gained some interest in other fields of chemical and physical science, e.g. as catalytic active material<sup>45</sup> or due to its properties (hard, clear, chemically stable) for the development of optoelectronic devices or solid-state lasers.<sup>46</sup>

Due to the different behavior of single and polycrystalline material, the corresponding electrical properties will be separately discussed in the following sections for  $\beta$ - and  $\beta''$ -alumina compounds, respectively.

**5.2.1.  $M^{2+}$ - $\beta''$ -Alumina Single Crystals.** For investigating the basic knowledge of conduction processes, single crystals are the most suitable material because the conductivity is not influenced by grain boundaries. Furthermore, single crystals of  $\beta''$ -alumina compounds always exhibit a platelet-like habit with the  $c$ -axis perpendicular to the plate area and are easy to handle for electrical measurements. The electrodes can be attached visually to the crystals and no X-ray diffraction based adjustments are necessary to identify the required  $ab$ -plane for the conductivity measurements.

Although the diffusion of divalent ions is much slower than that of the monovalent cations, the  $Na^+$  content

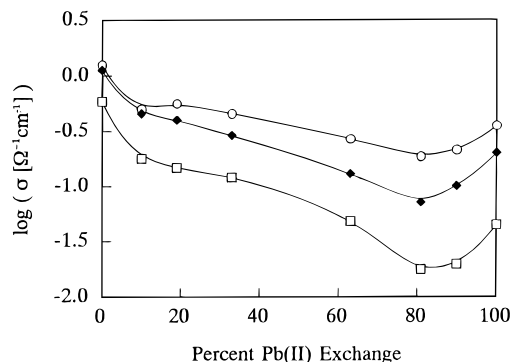


**Figure 4.** Ionic conductivity ( $\log \sigma$ ) as a function of the  $Pb^{2+}$  exchange in  $Na^+/Pb^{2+}$ - $\beta''$ - $Al_2O_3$  at three different temperatures: ○ = 350 °C; ◆ = 250 °C; □ = 150 °C. (Reproduced with permission from ref 53. copyright 1990 Academic Press.)

can be almost completely<sup>47</sup> replaced in  $Na^+$ - $\beta''$ - $Al_2O_3$  single crystals. Ion exchange reactions, which result in at least partially exchanged samples, have been reported for a various number of divalent cations, e.g., Ca,<sup>48–50</sup> Sr,<sup>27,48–50</sup> Ba,<sup>27,49–51</sup> Sn,<sup>43,52</sup> Pb,<sup>43,49,50,53,54</sup> Mn,<sup>43,55,56</sup> Co,<sup>43,56</sup> Ni,<sup>43,56</sup> Zn,<sup>55</sup> Cd,<sup>27,50</sup> Hg,<sup>57</sup> Eu.<sup>43,58–60</sup> As already mentioned, the ionic conduction in these  $M^{2+}$ - $\beta''$ -aluminas is always of complex nature. At low temperatures the divalent cations are fixed within their crystallographic positions and only the sodium ions transport the ionic current. Only at elevated temperatures are the divalent cations assumed to become mobile, leading to additional contributions for the ionic conductivity. Such a divalent cation transport in  $M^{2+}$ - $\beta''$ -alumina is already demonstrated in several distinct experiments, as will be shown in this section.

Compared to monovalent  $\beta''$ -aluminas with typical conductivity values between  $10^0$  and  $10^1 \Omega^{-1} cm^{-1}$  at 300 °C, the conductivity in divalent  $M^{2+}$ - $\beta''$ -aluminas is lowered by about 1–2 orders of magnitude at comparable temperatures combined with higher activation energies. Whereas  $M^{2+}$ - $\beta''$ - $Al_2O_3$  are poor conductors at room temperature, their conductivity increases remarkably at higher temperatures. Assuming mobile divalent cations, the raised activation energies are caused by stronger electrostatic interactions between the higher charged cations and the surrounding anionic oxygen lattice, which lead to reduced mobilities and thus decreased conductivity data.

To identify the nature of the mobile species, the conduction behavior for different  $Na^+/M^{2+}$  concentration ratios (different degree of exchange) has been estimated for several  $Na^+/M^{2+}$ - $\beta''$ - $Al_2O_3$ . As an example, the ionic conduction behavior in the  $Na^+/Pb^{2+}$ - $\beta''$ - $Al_2O_3$  system is considered. Highly exchanged  $Pb^{2+}$ - $\beta''$ - $Al_2O_3$  is found to exhibit the highest conductivity ( $\sigma \approx 10^{-1} \Omega^{-1} cm^{-1}$  at 300 °C) among the single crystalline  $M^{2+}$ - $\beta''$ -aluminas.<sup>53</sup> Measurements of the dependence of conductivity on the crystal composition (degree of exchange), as shown in Figure 4, indicate a divalent  $Pb^{2+}$  migration. The degree of exchange of the samples are well-determined from weight change as well as from <sup>22</sup>Na radioactive tracer activity measurements. Referring to Figure 4, the conductivity gradually decreases with increasing  $Pb^{2+}$  content and passes through a minimum at around 80%  $Na^+$  replacement. Theoretically, a continuous decrease of the conductivity across the whole composition range would be expected due to the sub-

stitution of highly mobile  $\text{Na}^+$  ions with less mobile divalent  $\text{Pb}^{2+}$  cations (decrease in average mobility). However, the nonlinear decline indicates a more complex behavior that is explained by ion-vacancy correlations in the conduction planes. As the degree of the ion-vacancy order increases, the movement of the mobile cations is more and more correlated. A high correlation is connected to higher activation energies (for breaking up the correlated structures) and thus with lower conductivities at a given temperature. By tuning the ion-vacancy ratio ( $\text{Na}^+$  replacement by divalent cations), there should exist a point with a maximal ordering of the mobile ion sublattice which is connected to the minimum in ionic conductivity. From computer-based simulations using Monte Carlo methods (assuming an overall mobility of all cations in the conduction planes), it is found that in crystals where 50% of the BR sites are occupied, maximum correlation effects by the formation of ion-vacancy pairs exist which in turn cause a minimum in conductivity.<sup>61</sup> Concerning  $\text{Na}^+/\text{Pb}^{2+}-\beta''\text{-Al}_2\text{O}_3$  crystals, this situation corresponds to a composition with approximately 80%  $\text{Na}^+$  replacement, which is in excellent agreement with the observations given in Figure 4. Assuming only  $\text{Na}^+$  ions as mobile cations and  $\text{Pb}^{2+}$  cations as fixed in the crystal structure, the conductivity should exhibit a different behavior in dependence on the crystal composition. Furthermore, if the  $\text{Pb}^{2+}$  cations are immobile, a sharp decrease in ionic conductivity should be expected with an increasing degree of exchange, due to the drastically diminishing number of charge carriers and the blocking of the pathways by immobile  $\text{Pb}^{2+}$  cations. The observed gentle lowering in conductivity for crystals with an  $\text{Na}^+$  replacement of 10–50% is in contradiction to this expectation. More likely is the interpretation that additional conductivity contributions of the less mobile divalent  $\text{Pb}^{2+}$  cations lead to the observed smooth decline.

Another indication for divalent cationic conduction in  $\text{M}^{2+}-\beta''\text{-alumina}$  concerns the determination of the  $\text{Sr}^{2+}$  diffusion coefficient ( $D_{\text{Sr}^{2+}}$ ) in ion-exchanged  $\text{Sr}^{2+}-\beta''\text{-Al}_2\text{O}_3$  crystals from radiotracer experiments.<sup>49</sup> The measured diffusion coefficient was used in the Nernst–Einstein equation to calculate a theoretical value for the conductivity  $\sigma_{\text{theo}}$ ,

$$\sigma_{\text{theo}} T = \frac{nq^2 D_{\text{Sr}^{2+}}}{k} \quad (2)$$

where  $n$  denotes the carrier density of the  $\text{Sr}^{2+}$  cations,  $q$  their charge, and  $k$  the Boltzmann constant. The calculated conductivity is in good agreement with conductivity data obtained by impedance spectroscopy. This result leads to the conclusion that  $\text{Sr}^{2+}$  cations are the predominant charge carriers in  $\text{Sr}^{2+}-\beta''\text{-Al}_2\text{O}_3$  and that their motion is sufficiently rapid to account for the observed conductivity. Residual  $\text{Na}^+$  cations or protons seem not to remarkably influence the conduction behavior of the divalent cationic charge carrier. The results of this experiment are of fundamental consequence since they demonstrate the correspondence between the migration of mobile divalent cationic species in a chemical potential gradient and an electric field gradient.

As already mentioned, computer-based calculations to simulate ionic conduction features in multivalent  $\beta''\text{-alumina}$  are a further helpful tool for the verification of multivalent cationic conduction processes, such as Monte Carlo methods<sup>61,62</sup> or molecular dynamics modeling.<sup>51,63</sup> Partially exchanged  $\text{Na}^+/\text{M}^{n+}-\beta''\text{-Al}_2\text{O}_3$  are appropriate candidate compounds for these calculations. They contain two different kinds of cations within the conduction planes, and the conduction behavior can be investigated with changing crystal composition, i.e., with changing  $\text{Na}^+/\text{M}^{n+}$  ratio. To maintain charge neutrality during the ion exchange reaction, one divalent (trivalent) cation replaces two (three) monovalent  $\text{Na}^+$  cations by the simultaneous creation of one (two) additional vacancies. Thus, the ion–ion correlations and the cation-vacancy ratio in the conduction planes are tunable by the degree of exchange which in turn is adjustable by controlling the exchange conditions, like temperature, time, etc. The observed experimental data for both divalent  $\text{Na}^+/\text{M}^{2+}-\beta''\text{-Al}_2\text{O}_3$ <sup>53,63</sup> and trivalent  $\text{Na}^+/\text{M}^{3+}-\beta''\text{-Al}_2\text{O}_3$  systems<sup>63</sup> could be well-simulated (at least qualitatively) by assuming multivalent cationic migration in the theoretical calculations.

Considering all experimental data presented in the previous section, the divalent cationic conduction is strongly indicated to occur in  $\text{M}^{2+}-\beta''\text{-Al}_2\text{O}_3$  compounds and only little doubt can remain concerning the mobility of divalent cationic charge carriers in these crystalline materials.

*5.2.2. Polycrystalline  $\text{M}^{2+}-\beta''\text{-Alumina}$ .* Whereas single crystals are the most appropriate materials to investigate the fundamentals of the electrical conduction, polycrystalline material is of greater interest for the development of electric applications. Single crystals are limited in size and not suitable to deform or to adjust into a required shape for particular technical devices. Therefore, many efforts have been undertaken after the first divalent ion exchange into  $\text{Na}^+-\beta''\text{-alumina}$  in 1969<sup>26</sup> to synthesize various kinds of polycrystalline divalent  $\text{M}^{2+}-\beta''\text{-Al}_2\text{O}_3$ , e.g.,  $\text{M} = \text{Ca}$ ,<sup>64–68</sup>  $\text{Sr}$ ,<sup>64,65,69–72</sup>  $\text{Ba}$ ,<sup>64,65,69</sup>  $\text{Cd}$ ,<sup>64,65,69</sup>  $\text{Sn}$ ,<sup>64,65</sup>  $\text{Pb}$ ,<sup>64,65,71–73</sup>  $\text{Zn}$ ,<sup>64,65,74</sup>  $\text{Ni}$ ,<sup>64,74</sup>  $\text{Mn}$ ,<sup>75</sup>  $\text{Hg}$ ,<sup>57,75</sup> and  $\text{Eu}$ .<sup>76,77</sup> But unfortunately, the investigation of polycrystalline material encountered several serious problems which do not appear in single crystals.

*(1) The Preparation by Ion Exchange Methods, Especially by the Molten Salt Technique.* Experimental difficulties arise from the elevated temperatures which are required for fusing the high-melting halide/nitrate salts (also observed for a monovalent cation exchange reactions).<sup>78</sup> Adhering salt residuals in the pores between the  $\beta''\text{-alumina}$  grains after the ion exchange cause misinterpretations of weight change measurements for the determination of the degree of exchange. In addition, these salt residuals can influence the electrical measurements by additional conductivity contributions, even at higher temperatures where the divalent cations are assumed to migrate. Further problems concern the formation of cracks, the corrosion, and the etching of the polycrystalline sample in the molten salts. High porosity and the loss of grain material result, complicating the weight change determinations. The increased porosity causes contact problems in the electrical measurements when using solid

blocking electrodes. Additional difficulties are reported due to the thermal instability of  $\text{Na}^{+}\text{-}\beta''\text{-Al}_2\text{O}_3$ , which is observed to deteriorate (sometimes indicated by coloration) by degradation into e.g.  $\beta$ -alumina or magnetoplumbite-type compounds at higher temperatures. These complications can also lead to misinterpretations of the measured conductivity data.

(2) *Experimental Problems Concerning the Electrical Measurements.* The electrical properties of polycrystalline  $\text{Na}^{+}/\text{M}^{n+}\text{-}\beta''\text{-Al}_2\text{O}_3$  (and  $\text{Na}^{+}/\text{M}^{n+}\text{-}\beta\text{-Al}_2\text{O}_3$ ) samples do not only depend on the bulk ionic conductivity but are also influenced by extrinsic factors, such as grain boundaries, the alignment of conduction planes across grain boundaries, the presence of second phases, microcracks, and interfacial electrode processes. As these factors may vary from sample to sample, the conductivity data are not reproducible and a comparison between different polycrystalline compounds (i.e. between samples characterized in different laboratories) is difficult.

(3) *The Conduction Properties are Significantly Decreased.* As a general trend, the conductivity in polycrystalline  $\text{M}^{2+}\text{-}\beta''\text{-Al}_2\text{O}_3$  compounds is in the range of  $\sigma = 10^{-7}\text{--}10^{-3} \Omega^{-1} \text{cm}^{-1}$  (for  $T = 300\text{--}500 \text{ }^\circ\text{C}$ ), which is lower by several orders of magnitude in comparison to corresponding single-crystal data ( $\sigma_{300\text{--}500 \text{ }^\circ\text{C}} = 10^{-3}\text{--}10^{-1} \Omega^{-1} \text{cm}^{-1}$ ). In polycrystalline material, the particles are randomly orientated, generating isotropic conduction in contradiction to the two-dimensional character of single crystals. The alignment of the conduction slabs between two adjacent grains does not necessarily match, leading to an interruption of the pathways for the mobile ions, which in turn reduces the total amount of the ionic conductivity.

The potential use as solid electrolytes in technical devices has led to a more thorough investigation of polycrystalline material, in comparison to single crystals. Even with regard to the nature of the charge carrier, the electrical properties of polycrystals have been characterized in more detail. For example, the electronic contributions to the total electrical conductivities are determined (e.g., by Wagner's polarization method) to ensure the ionic conduction character. They are about 2–3 orders of magnitude lower than the total electrical conductivities (electronic transference number is less than 0.01). Thus, these materials can be regarded as pure ionic conductors. To verify the cationic or anionic nature of the mobile species, electromotive force (EMF) measurements have been performed in various kinds of galvanic cells using polycrystalline  $\text{M}^{2+}\text{-}\beta''\text{-Al}_2\text{O}_3$  as solid electrolyte.<sup>74,75</sup> In these measurements the standard free energies for the formation of compounds at the electrodes according to the cell reactions are calculated from the observed EMF values and compared with known thermodynamic data from the literature. The agreement between both data verifies the assumed cell reactions and leads to the conclusion of an overall mobility of the regarded charge carrier species within the solid electrolyte. As an example, in the oxide galvanic cell

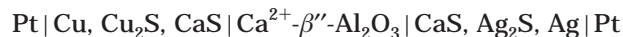


using ion-exchanged  $\text{Mn}^{2+}\text{-}\beta''\text{-Al}_2\text{O}_3$ , the standard free enthalpy change for the cell reaction  $\text{MnO} + \text{Mn}_2\text{O}_3 = \text{Mn}_3\text{O}_4$  was estimated as  $\Delta G = 29.68 \text{ kJ/mol}$ ,<sup>75</sup> which is

in very good accordance with corresponding literature data ( $\Delta G^\circ = 29.949 \text{ kJ/mol}$ ). The exclusive ionic current transport could be confirmed by measuring a negligible electronic transference number ( $t_{el} < 10^{-3}$ ). Thus,  $\text{Mn}^{2+}$  cations are strongly expected to be the predominant mobile charge carriers in  $\text{Mn}^{2+}\text{-}\beta''\text{-Al}_2\text{O}_3$ . However, some problems are connected with the reported experimental setup, which might bring into question the observed results. One difficulty concerns the oxidation state of the manganese cations. Since manganese (or other transition and rare earth metals) can adopt different valences, the exclusive divalent oxidation state must be ensured during the exchange reaction and during the electrical measurements. In the case of the simultaneous presence of  $\text{Mn}^{n+}$  cations in different valence states, the EMF data measured in the above-mentioned experiment become meaningless. But since  $\beta$ -alumina tend to reduce rather than to oxidize incorporated cations, there is a high probability for the exclusive divalent character of the manganese cations.

The other problem concerns the unknown effects of remaining  $\text{Na}^{+}$  and/or  $\text{O}^{2-}$  ions and/or protons on the observed experimental data. Since these charge carrier cannot be reliably excluded, the measured EMF may not be purely attributed to the migration of  $\text{Mn}^{2+}$  cations, leading to some uncertainty in the interpretation. Nevertheless, these EMF measurements on polycrystalline material provide another strong indication for the divalent cation transport in ion-exchanged  $\text{M}^{2+}\text{-}\beta''\text{-Al}_2\text{O}_3$ , which in addition to the experiments on single crystalline material leads to a comprehensive insight into this phenomenon.

Measurements on the electrical properties are also available for polycrystalline  $\text{M}^{2+}\text{-}\beta''\text{-Al}_2\text{O}_3$  material that has been prepared by direct synthesis. For example,  $\text{Ca}^{2+}\text{-}\beta''\text{-Al}_2\text{O}_3$  has been prepared from a mixture of  $\text{CaCO}_3$ ,  $\text{MgCO}_3$ , and  $\alpha\text{-Al}_2\text{O}_3$  at calcination and sintering temperatures of about 1000 and 1650  $^\circ\text{C}$ , respectively.<sup>68,79</sup> Since this compound should not contain any amount of sodium ions (besides the impurities of the reagents), the electrical properties only depend on the migration properties of the divalent  $\text{Ca}^{2+}$  ions (as far as cationic conduction is concerned). Using  $\text{Ca}^{2+}\text{-}\beta''\text{-Al}_2\text{O}_3$  as electrolyte in the calcium concentration cell



the conduction behavior and thus the ability for  $\text{Ca}^{2+}$  migration is deducible. The measured EMF in this cell arises as a result of the sulfur partial pressure difference at the two electrodes.<sup>79</sup> In Figure 5, the observed EMF data are shown in comparison with theoretical data taken from the literature. Due to the remarkable agreement, the conclusion can be drawn that  $\text{Ca}^{2+}$  ions represent the mobile charge carriers with an ionic transference number of unity. Similar data have been obtained in other galvanic cells utilizing  $\text{Ca}^{2+}\text{-}\beta''\text{-Al}_2\text{O}_3$  as a solid electrolyte.<sup>80</sup> As a critical point similar to the aforementioned example ( $\text{Mn}^{2+}\text{-}\beta''\text{-Al}_2\text{O}_3$ ), the possibility of another mobile charge carrier (protons,  $\text{O}^{2-}$  or  $\text{S}^{2-}$  anions, or other cationic impurities) which may also respond to the electromotive force in that electric cell cannot be excluded until corresponding measurements have been performed. But due to the excellent agree-

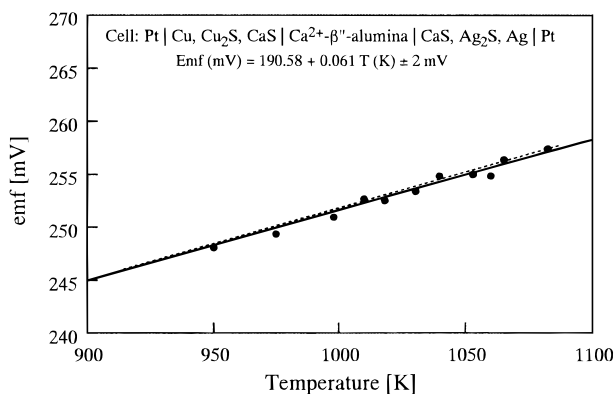


**Figure 5.** Characterization of  $\text{Ca}^{2+}\text{-}\beta''\text{-Al}_2\text{O}_3$  solid electrolyte for divalent cationic conduction. The electromotive force of the galvanic cell is shown as a function of the temperature. The solid line represents the linear regression for the observed data, whereas the broken line corresponds to theoretical literature data. Reproduced with permission from ref 79. Copyright 1985 the Metallurgical Society.

ment between experimental and theoretical data, there remains only a small probability for a misinterpretation.

Assuming a predominant  $\text{Ca}^{2+}$  transport in  $\text{Ca}^{2+}\text{-}\beta''\text{-Al}_2\text{O}_3$ , these experiments are also useful to investigate and to compare effects on the electrical conduction which are due to a residual sodium amount (due to impurities) in ion-exchanged (direct synthesized) samples. Ion-exchanged  $\text{Ca}^{2+}\text{-}\beta''\text{-Al}_2\text{O}_3$ , used as solid electrolyte in the same electric cells under identical conditions, is expected to produce similar results if the influence of the remaining  $\text{Na}^+$  ions (or impurities) is negligible. However, these data are not available yet.

Further information about possible effects of residual sodium ions can be gained from the comparison between the electrical conduction data (measured by impedance spectroscopy) of  $\text{Ca}^{2+}\text{-}\beta''\text{-Al}_2\text{O}_3$  prepared either by ion exchange or by direct synthesis. Table 2 shows that the conductivity in the sample prepared by direct synthesis is slightly lowered, whereas the activation energy is increased. This behavior can be interpreted in terms of present residual  $\text{Na}^+$  ions in the ion-exchanged sample, which lead to additional conductivity contributions and therefore to a higher observed conductivity and lower activation energy. This observation suggests that the remaining sodium ions in highly exchanged  $\text{M}^{2+}\text{-}\beta''\text{-Al}_2\text{O}_3$  do have an effect on the conduction behavior which cannot be neglected. However, it must be pointed out that the comparison between these two data is unreliable, due to different experimental conditions (electrodes, porosity, etc.) and due to missing information about the purity of the reagents used. But despite this uncertainty, the data are shown here, to raise the sensibility for the interpretation of conductivity data in  $\text{M}^{n+}\text{-}\beta''\text{-Al}_2\text{O}_3$ .

In conclusion, the  $\text{M}^{2+}\text{-}\beta''\text{-Al}_2\text{O}_3$  are already well-characterized compounds with regard to their divalent conduction properties. Only data from dc electrolysis experiments are still missing, which would lead to an unambiguous identification of the charge carrier.

**5.2.3.  $\text{M}^{2+}\text{-}\beta\text{-Alumina. Single Crystals.}$**  As for  $\text{Na}^+\text{-}\beta\text{-Al}_2\text{O}_3$ , the sodium content in  $\text{Na}^+\text{-}\beta\text{-Al}_2\text{O}_3$  can also be replaced by a various number of other cations. However, the exchange behavior between both phases significantly differs, reflecting the different ionic con-

**Table 2. Comparison of the Electrical Conductivity ( $\sigma$ ) at 450 °C and the Corresponding Activation Energy ( $E_a$ ) of  $\text{Ca}^{2+}\text{-}\beta''\text{-Al}_2\text{O}_3$  Prepared by Ion Exchange and by Direct Synthesis**

$\text{Ca}^{2+}\text{-}\beta''\text{-Al}_2\text{O}_3$	$\sigma_{450^\circ\text{C}}$ [ $\Omega^{-1}\text{cm}^{-1}$ ]	$E_a$ [eV]	ref
ion exchange	$3.9 \cdot 10^{-3}$	0.49	66
direct synthesis	$1.2 \cdot 10^{-4}$	$\approx 0.71$	68

duction properties.  $\text{Na}^+\text{-}\beta''\text{-Al}_2\text{O}_3$  is 2–3 times higher in ionic conduction than  $\text{Na}^+\text{-}\beta\text{-Al}_2\text{O}_3$  and easier to ionically exchange, especially for the case of multivalent cations. These cations are found to diffuse faster into the conduction planes of  $\text{Na}^+\text{-}\beta''\text{-Al}_2\text{O}_3$  leading to a nearly complete ion exchange at lower temperatures ( $T_{\text{ex}}$ ) or shorter reaction times ( $t_{\text{ex}}$ ). For example, after the ion exchange reaction in a  $\text{Ba}(\text{NO}_3)_2/\text{BaCl}_2$  salt mixture using similar conditions ( $T_{\text{ex}} = 550^\circ\text{C}$ ,  $t_{\text{ex}} = 20$  h), an almost complete ion exchange was observed for  $\text{Na}^+\text{-}\beta''\text{-Al}_2\text{O}_3$  crystals, whereas only 5% of the  $\text{Na}^+$  content was replaced by  $\text{Ba}^{2+}$  cations in  $\text{Na}^+\text{-}\beta\text{-Al}_2\text{O}_3$  single crystals within the same time.<sup>28,50</sup>

The different ion exchange and ionic conduction behavior between  $\beta''$ - and  $\beta$ -aluminas is assumed to be due to different atomic arrangements in the conduction planes and due to different conduction mechanisms in the two phases.<sup>28</sup> For example, the ionic conduction in unexchanged  $\text{Na}^+\text{-}\beta\text{-Al}_2\text{O}_3$  with the general composition  $\text{Na}_{1+x}\text{Al}_{11}\text{O}_{17+x/2}$  occurs by an interstitialcy process for which a nonstoichiometric excess ( $x$ ) of  $\text{Na}^+$  ions are essential.<sup>81</sup> Usually, BR sites are the favorable positions for the cations to occupy within the conduction planes of  $\text{Na}^+\text{-}\beta\text{-Al}_2\text{O}_3$ . If  $x = 0$  in  $\text{Na}_{1+x}\text{Al}_{11}\text{O}_{17+x/2}$ , all sodium ions are trapped within deep potential wells at these BR sites and the ionic conduction can only occur by a high activation energy. Excessive cations ( $x > 0$ ) are found to occupy the interstitial aBR (anti-Beevers–Ross) or mO sites which are connected with a low activation energy for the ionic migration process. Thus, the ionic conduction in unexchanged  $\text{Na}^+\text{-}\beta\text{-Al}_2\text{O}_3$  is carried by these interstitial  $\text{Na}^+$  cations. Due to the numerous reduction of  $\text{Na}^+$  ions during the ion exchange with multivalent cations, all cations in the conduction planes occupy the favorable BR positions and the interstitialcy conduction process can no longer be maintained. In consequence, the mobility and hence the ion exchange ability is drastically lowered. On the contrary, the ionic conduction in  $\text{Na}^+\text{-}\beta''\text{-Al}_2\text{O}_3$  occurs by a vacancy mechanism. BR and aBR sites are equivalent in  $\text{Na}^+\text{-}\beta''\text{-Al}_2\text{O}_3$  (only referred to as BR sites) and numerically exceed the number of cations. Multivalent cation substitution only increases the total vacancy population but does not change the conduction mechanism as in  $\text{Na}^+\text{-}\beta\text{-Al}_2\text{O}_3$ , and the ability for the comparatively easy ion replacement remains unchanged. This simplified model has already been confirmed by X-ray investigations in the  $\text{Na}^+/\text{Cd}^{2+}\text{-}\beta\text{-Al}_2\text{O}_3$  system<sup>82</sup> as well as by theoretical molecular-dynamics simulations.<sup>83</sup>

Due to the significantly lower diffusion rates, only a few papers report on the preparation and electrical properties of highly exchanged divalent  $\text{M}^{2+}\text{-}\beta\text{-aluminas}$ .<sup>82,84–87</sup> In comparison to other divalent cations,  $\text{Cd}^{2+}$  appears to be the only cation to replace  $\text{Na}^+$  nearly completely and more rapidly in  $\text{Na}^+\text{-}\beta\text{-Al}_2\text{O}_3$  single crystals. The reason for this behavior is not known yet. Conductivity data of mixed  $\text{Na}^+/\text{Cd}^{2+}\text{-}\beta\text{-}$

$\text{Al}_2\text{O}_3$  crystals have been found in the literature only for low temperatures ( $T < 600$  °C) where the  $\text{Cd}^{2+}$  ions are assumed to be trapped in the structure and therefore do not contribute to the conductivity.<sup>84</sup> No other reports on conductivity measurements on highly exchanged  $\text{M}^{2+}$ - $\beta$ - $\text{Al}_2\text{O}_3$  have been published. It is not possible to check the migration properties of divalent cations in  $\text{M}^{2+}$ - $\beta$ - $\text{Al}_2\text{O}_3$  single crystals in detail, since the conductivity data in the mixed compounds are mainly caused by mobile sodium ions. But the possibility of a partial ion exchange at elevated temperatures gives at least some positive indications for the occurrence of this phenomenon.

**Polycrystals.** Ion exchange reactions with divalent cations in polycrystalline  $\text{Na}^+$ - $\beta$ - $\text{Al}_2\text{O}_3$  have been reported for Cd,<sup>84,88</sup> Zn,<sup>89</sup> Ni,<sup>90,91</sup> Ca,<sup>92</sup> Sr,<sup>92-94</sup> Ba,<sup>92,93</sup> Fe,<sup>95</sup> Cu,<sup>96</sup> and Eu.<sup>76</sup> In principle, the similar exchange properties and difficulties as in polycrystalline  $\text{Na}^+$ - $\beta$ - $\text{Al}_2\text{O}_3$  are observed for the  $\beta$ -phase. Polycrystalline material is much more difficult to ionically exchange than single crystals, and in most cases only a partial substitution could be achieved. Some of these partially exchanged polycrystalline  $\text{M}^{2+}$ - $\beta$ - $\text{Al}_2\text{O}_3$  materials have been used as solid electrolytes in oxide galvanic cells for the measurements of thermodynamic properties.<sup>91,95,96</sup> The reasonable agreement of the experimental thermodynamic data with literature data indicates the migration properties of the divalent cations.

In contradiction to the  $\beta'$ -phases, divalent  $\text{M}^{2+}$ - $\beta$ - $\text{Al}_2\text{O}_3$  compounds are more easily accessible by direct synthesis methods. Several examples of the successful preparation by this technique are given in the literature.<sup>92-94</sup> The electrical properties of these materials can be interpreted rather in terms of divalent cationic motions due to the absence of sodium ions (except the impurities). However, the cationic diffusion is significantly low. The conductivities are several orders of magnitude lower than in polycrystalline  $\text{M}^{2+}$ - $\beta'$ - $\text{Al}_2\text{O}_3$ . Typical values are  $10^{-4}$ – $10^{-6}$   $\Omega^{-1}$   $\text{cm}^{-1}$  at 730 °C, whereas the same data are already observed at temperatures around 300–400 °C in  $\text{M}^{2+}$ - $\beta'$ -polycrystals.

In conclusion, the electrical properties of divalent  $\text{M}^{2+}$ - $\beta$ - $\text{Al}_2\text{O}_3$  are not well established in detail and not supported by numerous investigations as in the case of  $\text{M}^{2+}$ - $\beta'$ - $\text{Al}_2\text{O}_3$ . This may be due to the difficulties in preparing pure, i.e., highly exchanged, divalent  $\text{M}^{2+}$ - $\beta$ - $\text{Al}_2\text{O}_3$  material. The characterization of a divalent cationic current transport is still incomplete and requires further investigation to clearly verify  $\text{M}^{2+}$ - $\beta$ - $\text{Al}_2\text{O}_3$  compounds as divalent cationic conductors.

**5.3.  $\text{M}^{2+}\text{Zr}_4(\text{PO}_4)_6$ .** Besides the  $\beta$ -Alumina family, there exists another huge group of ion conducting compounds built up by a zirconium phosphate lattice which is intersected by open tunnels and/or layers hosting monovalent as well as divalent cations. The famous representative compound of this group is the  $\text{Na}^+$  super ionic conductor NASICON ( $\text{Na}_{1+x}\text{Zr}_2\text{P}_3-x\text{Si}_x\text{O}_{12}$ ,  $0 \leq x \leq 3$ ) which was synthesized and electrically characterized in 1976.<sup>97,98</sup> The zirconium phosphate framework is well-known for its ability to host mobile monovalent cations (e.g.  $\text{Na}^+$ ,  $\text{Li}^+$ ) and many of the compounds derived from NASICON exhibit excellent ionic conduction behaviors. As for  $\beta$ -Alumina, some efforts to create new types of solid electrolytes are based

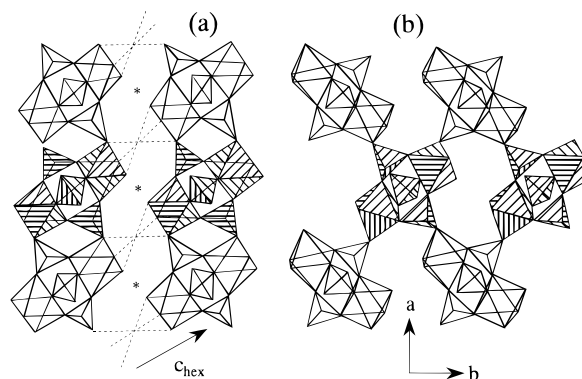


**Figure 6.** Simplified schematic figures for the comparison of the crystal structure types of (a) NASICON with the projection along the rhombohedral  $a$ -axis and (b)  $\beta$ - $\text{Fe}_2(\text{SO}_4)_3$  with a projection in the (001) plane of the monoclinic unit cell. To give a better impression for the different connection of the  $[\text{A}_2(\text{XO}_4)_3]^-$  units, some parts of the frameworks are omitted and some are hatched. In panel a, the  $\text{M}_1$  site lies in the intersection points of the (---) lines, and asterisks roughly denote the positions of the  $\text{M}_2$  sites.

on the idea of replacing the monovalent cations in the NASICON related materials by cations in a divalent oxidation state. New compounds  $[\text{M}^{2+}\text{Zr}_4(\text{PO}_4)_6]$  could be synthesized by adopting the NASICON or the related  $\beta$ - $\text{Fe}_2(\text{SO}_4)_3$  structure type but containing divalent cations. However, in contradiction to divalent  $\beta$ -Alumina, which have been mostly prepared by ion exchange reaction starting from monovalent material, the divalent phosphate compounds are obtained by direct synthesis in sol-gel methods using  $\text{M}^{2+}(\text{NO}_3)_2 \cdot n\text{H}_2\text{O}$ ,  $\text{ZrOCl}_2 \cdot 8\text{H}_2\text{O}$  or  $\text{ZrO}(\text{NO}_3)_2 \cdot 2\text{H}_2\text{O}$ , and  $\text{NH}_4\text{H}_2\text{PO}_4$  as starting reagents.<sup>99-101</sup>

The  $\text{M}^{2+}$  cations are found to be mobile in these  $\text{M}^{2+}$ - $\text{Zr}_4(\text{PO}_4)_6$  compounds at higher temperatures ( $T > 500$  °C). But in comparison to divalent  $\text{M}^{2+}$ - $\beta$ - or  $\text{M}^{2+}$ - $\beta'$ -aluminas, the divalent zirconium phosphates are significantly lower in electrical conduction. Depending on the ionic size, the NASICON-type structure is observed for  $\text{M}^{2+}\text{Zr}_4(\text{PO}_4)_6$  with larger M (Ca, Sr, Ba, Cd, Pb, Mn), whereas  $\text{M}^{2+}\text{Zr}_4(\text{PO}_4)_6$  with smaller M (Mg, Co, Ni, Zn, Mn) crystallizes in the  $\beta$ - $\text{Fe}_2(\text{SO}_4)_3$ -type structure. The Mn compound forms both structure types, depending on the synthesis conditions. Figure 6 compares both the NASICON and  $\beta$ - $\text{Fe}_2(\text{SO}_4)_3$ -type crystal structures. In the rhombohedral NASICON structure type,  $\text{XO}_4$  ( $\text{X} = \text{P}, \text{Si}$ ) tetrahedra are linked by corner-sharing with  $\text{AO}_6$  ( $\text{A} = \text{Zr}$ ) octahedra forming a three-dimensional skeleton structure built up by  $[\text{A}_2(\text{XO}_4)_3]^-$  units in which each O atom is bonded to only one X and one A atom. An  $\text{AO}_6$  octahedron is connected to six  $\text{XO}_4$  tetrahedra, while each tetrahedron is linked to four octahedra. A three-dimensional network of tunnels results in which the conducting ions can occupy two distinct sites, usually labeled as  $\text{M}_1$  and  $\text{M}_2$  positions.<sup>97,98</sup> The monoclinic  $\beta$ - $\text{Fe}_2(\text{SO}_4)_3$  structure is similar to the NASICON structure, but the arrangement of the  $[\text{A}_2(\text{XO}_4)_3]^-$  units is altered.<sup>102</sup>

The electrical conduction behavior of the NASICON and the  $\beta$ - $\text{Fe}_2(\text{SO}_4)_3$ -type compounds differs due to the structural properties of the crystallographic positions where the cations are accommodated.<sup>100</sup> In the NASICON-type structure, mobile cations usually occupy the  $\text{M}_1$  sites, with elongated antiprisms sharing triangular

faces with the two adjacent  $\text{ZrO}_6$  octahedra along the  $c$ -axis of the hexagonal cell. The anisotropic separation of these two  $\text{ZrO}_6$  polyhedra in the  $c$ -direction determines the size of the bottleneck for the conduction pathway between the  $M_1$  and  $M_2$  positions.<sup>103,104</sup> The extension of this bottleneck is found to be dependent on the size of the mobile cation. Therefore, the ionic conductivity in the NASICON-type  $M^{2+}\text{Zr}_4(\text{PO}_4)_6$  compounds changes significantly with only slight variations in the size of the mobile ion. In contradiction,  $\beta\text{-Fe}_2(\text{SO}_4)_3$ -type compounds show only a slight dependence of the conductivity on the cationic radius.<sup>5</sup> In this crystal structure, mobile ions occupy 4-fold coordinated positions which isotropically expand upon increasing the diameter of the cations, and the alternation with the bottleneck size is less pronounced than in the NASICON structure.<sup>101,105</sup>

The conductivities of the  $M^{2+}\text{Zr}_4(\text{PO}_4)_6$  in the  $\beta\text{-Fe}_2(\text{SO}_4)_3$ -type structure are comparatively higher ( $\sigma_{800^\circ\text{C}} \approx 10^{-3} \Omega^{-1} \text{cm}^{-1}$ ) than the phosphates in the NASICON-type structure ( $\sigma_{800^\circ\text{C}} \approx 10^{-7}\text{--}10^{-4} \Omega^{-1} \text{cm}^{-1}$ ). Activation energies vary between 0.8 and 1.0 eV [ $\beta\text{-Fe}_2(\text{SO}_4)_3$ -type] and 1.5 and 5.2 eV (NASICON-type). The highest conductivity for a  $\beta\text{-Fe}_2(\text{SO}_4)_3$ -type compound is observed in  $\text{ZnZr}_4(\text{PO}_4)_6$  ( $\sigma_{800^\circ\text{C}} = 1.9 \cdot 10^{-3} \Omega^{-1} \text{cm}^{-1}$ ) and is seen for a NASICON-type compound in  $\text{MnZr}_4(\text{PO}_4)_6$  ( $\sigma_{800^\circ\text{C}} = 8.3 \cdot 10^{-4} \Omega^{-1} \text{cm}^{-1}$ ). The different conduction behavior in both structure types is due to the altered connection of the  $[\text{A}_2(\text{XO}_4)_3]^-$  building units, which provides more open pathways for mobile cations in the  $\beta\text{-Fe}_2(\text{SO}_4)_3$ -type structure.

To identify the charge carrier, a combination of polarization measurements and Tubandt electrolysis experiments has been performed. The ionic transference numbers ( $t_i$ ) of the compounds, determined by the polarization measurements, indicate an exclusively ionic migration in the  $\beta\text{-Fe}_2(\text{SO}_4)_3$ -type compounds ( $t_i > 99.9\%$ ) and a predominant ionic transport in the NASICON-type compounds ( $t_i > 85\%$ ).<sup>99</sup> The next step to verify the divalent cations as mobile charge carriers included the application of dc electrolysis experiments in the Tubandt setup from which the final evidence for the cationic migration properties could be extracted.<sup>99</sup> The weight changes of the anodic as well as cathodic samples accorded with theoretical data calculated from Faraday's law to 70–90% by assuming a divalent cationic transport through the samples. This conclusion was further supported by the detection (XRD) of metal oxide deposits on the cathodic surfaces. It can be concluded that divalent cations move during the electrolysis from the anodic to the cathodic pellet (weight changes), where they chemically react with the atmosphere to form the corresponding oxides (deposits on cathodic surface). Hence, compounds in the  $M^{2+}\text{Zr}_4(\text{PO}_4)_6$  systems can be regarded as predominantly ionic conductors containing divalent cations as mobile charge carriers.

Other compounds in the  $\text{Mg-Zr-PO}_4$  and  $\text{Zn-Zr-PO}_4$  system conducting divalent cations but differing from  $M^{2+}\text{Zr}_4(\text{PO}_4)_6$  in composition (altered M:Zr:PO<sub>4</sub> ratio) and crystal structure have been reported.<sup>106,107</sup> However, the highest ionic conductivities and lowest activation energies are always observed in the 1:4:6 (M:Zr:PO<sub>4</sub>) compounds crystallizing in the  $\beta\text{-Fe}_2(\text{SO}_4)_3$ -type

structure. Similar to the monovalent NASICON compounds, attempts have been made to replace  $(\text{PO}_4)^{3-}$  tetrahedra by  $(\text{SiO}_4)^{4-}$  units.<sup>108</sup> Such a substitution is expected to enlarge the bottlenecks along the pathways between  $M_1$  and  $M_2$  sites and thus to improve the electrical properties. Indeed, the conductivities are increased by about 2 orders of magnitude, but from XRD measurements the formation of a second phase,  $\text{Zr}_2\text{O}(\text{PO}_4)_2$ , is observed. Thus, the enhancement in conductivity should be discussed in terms of a composite effect (heterogeneous doping) rather than by homogeneous doping.

In comparison to NASICON and its monovalent derivatives, the group of divalent  $M^{2+}\text{Zr}_4(\text{PO}_4)_6$  compounds represents a new family of solid electrolyte materials with divalent cationic conduction properties. Besides the  $\beta$ -Alumina materials, these compounds are further examples of how to use the crystal structure of fast monovalent cation conductors as a host lattice for multivalent cations in order to create new solid electrolyte materials. This concept seems to be very useful, even with respect to trivalent cation containing zirconium phosphates. As an example, the preparation of  $\text{Ln}^{3+}\text{Zr}_6(\text{PO}_4)_9$  (Ln = rare earth) crystallizing in the NASICON-type structure has been reported, recently.<sup>109</sup> Unfortunately, no conductivity measurements have been applied. Thus, the question of whether these compounds are able to conduct trivalent cations remains unanswered.

**5.4. YPO<sub>4</sub>-Based Compounds.** Another family of materials for which a divalent cationic migration could be unambiguously identified is given by YPO<sub>4</sub>-based compounds. YPO<sub>4</sub> crystallizes in the zircon structure type ( $\text{ZrSiO}_4$ ) where yttrium ions are surrounded by eight oxygen anions of isolated PO<sub>4</sub> tetrahedra. Fairly large interstitial sites are available within this crystal structure which can be occupied by additionally incorporated aliovalent cations during the formation of YPO<sub>4</sub>-based solid solutions with other phosphate compounds ( $\text{M}^{n+}_{3/n}\text{PO}_4$ ,  $n < 3$ ). By this method, it is possible to introduce divalent cations into the three-dimensional framework of YPO<sub>4</sub>, creating divalent cationic conductors.

The preparation, characterization, and electrical measurements have been reported for solid solutions in the systems  $(\text{YPO}_4)_{1-x}(\text{Mg}_{3/2}\text{PO}_4)_x$  ( $x \leq 0.15$ ) and  $(\text{YPO}_4)_{1-x}(\text{Ca}_{3/2}\text{PO}_4)_x$  ( $x \leq 0.05$ ).<sup>110</sup> In comparison to the poorly conducting undoped YPO<sub>4</sub>, the electrical conductivity is considerably increased by several orders of magnitude up to  $1.2 \cdot 10^{-3} \Omega^{-1} \text{cm}^{-1}$  in  $\text{Y}_{0.95}\text{Ca}_{0.075}\text{PO}_4$  and  $5.0 \cdot 10^{-5} \Omega^{-1} \text{cm}^{-1}$  in  $\text{Y}_{0.85}\text{Mg}_{0.225}\text{PO}_4$  at 600 °C, respectively. The charge carriers in these compounds were determined by Tubandt electrolysis experiments, and X-ray powder diffraction analysis has been used to characterize the sample surfaces. For example, after the electrolysis of  $\text{Y}_{0.95}\text{Ca}_{0.075}\text{PO}_4$ , white deposits were found on the cathodic surface (of the cathodic sample) and identified as calcium oxide, indicating a  $\text{Ca}^{2+}$  movement through the sample during the electrolysis. This indication was confirmed by weight change measurements of the anodic and cathodic sample pellets. According to Faraday's law, the actual weight loss for the anodic sample and the weight gain for the cathodic sample correspond to the theoretical values assuming  $\text{Ca}^{2+}$  migration and the

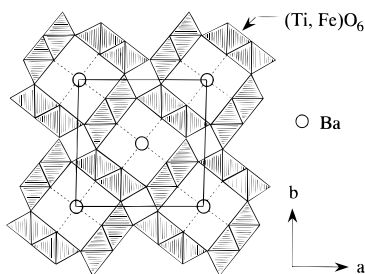


**Figure 7.** Schematic representation of the hollandite-type crystal structure with a projection along the  $c$ -axis. The unit cell is indicated by solid lines. In  $\text{Ba}_x\text{Ti}_{4-2x}\text{Fe}_{2x}\text{O}_8$  ( $x = 0.67$ ) the central positions of the tunnels, formed by  $(\text{Ti}, \text{Fe})\text{O}_6$  octahedra, are occupied by  $\text{Ba}^{2+}$  ions (indicated by opened circles) to 67%.

formation of  $\text{CaO}$ . Ionic transference numbers of 0.85–0.95 were calculated from these results.

It can be stated that compounds in the  $(\text{YPO}_4)_{1-x}(\text{M}_{3/2}\text{PO}_4)_x$  systems ( $\text{M} = \text{Mg}, \text{Ca}$ ) are divalent solid electrolytes with  $\text{Ca}^{2+}$  or  $\text{Mg}^{2+}$  cations as mobile divalent charge carriers, respectively. The investigations on these compounds demonstrate (similar to doped  $\text{CaS}$ ) how to increase the electrical conducting properties and how to create new solid electrolyte materials by aliovalent doping of low conducting compounds.

**5.5. Hollandite.** Some compounds of the hollandite family are reported to be cationic conductors. Although reasonable conductivities can only be found for the monovalent cation containing compounds, there are some reports concerning possible migration properties of divalent cations.

Hollandites are derived from the mineral  $\text{Ba}_x\text{Mn}_8\text{O}_{16}$  ( $x \leq 2$ ) to give in general  $\text{A}_x\text{B}_8\text{O}_{16}$ , with A being a large ion such as  $\text{Ba}^{2+}$ ,  $\text{Pb}^{2+}$ , or  $\text{K}^+$  and B being a small or medium-sized ion such as  $\text{Mn}^{4+}$ ,  $\text{Fe}^{3+}$ , or  $\text{Mn}^{2+}$ . The schematic crystal structure of a hollandite phase is shown in Figure 7. Within a tetragonal or pseudotetragonal framework of  $\text{MnO}_6$  octahedra sharing corners and edges, isolated square tunnels parallel to the crystallographic  $c$ -axis are formed hosting the A cations in a cubic coordination sphere.<sup>111,112</sup> Usually, the occupation of A cations within the tunnels is only partial and the charges are compensated by a mixed valency of B ions. As one of the disadvantages, these compounds are most often found to be mixed conductors with considerable electronic conductivity contributions, which prevent them from extended use as solid electrolyte materials in technical applications. On the basis of this hollandite structure, a large number of compounds differing in A and B exists. The opened tunnels along the  $c$ -direction seem to be interesting from the viewpoint of multivalent cationic conduction, and fast ion conducting properties were expected since the discovery of these compounds. But corresponding investigations always gave disappointing results. X-ray single diffraction studies reveal strong short-range order correlations between the A cations, which usually prohibit the hollandites from being used as suitable electrolyte materials, especially for compounds containing multivalent A cations.<sup>113</sup>

Titanium based mixed oxides  $\text{A}_x(\text{B}, \text{Ti})_8\text{O}_{16}$  (A, alkaline metal; B, Mg, Al, Ga, Fe, etc.), the so-called priderites, are isostructural with the hollandites and exhibit one-dimensional ionic conduction (monovalent cations) along

the tunnels.  $\text{Ba}_x\text{Ti}_{4-2x}\text{Fe}_{2x}\text{O}_8$  ( $x = 0.67$ ) in the ternary system  $\text{BaO}-\text{TiO}_2-\alpha\text{-Fe}_2\text{O}_3$  is an example of a divalent priderite compound with a monoclinic crystal structure for which the dielectric properties were measured.<sup>114</sup> At lower temperatures ( $T < 120^\circ\text{C}$ ) the observed conductivity is interpreted to be of electronic origin due to a charge transfer between  $\text{Fe}^{2+}$  and  $\text{Fe}^{3+}$  ions. A dielectric relaxation at  $120^\circ\text{C}$  is attributed to atomic displacements of  $\text{Ba}^{2+}$  cations in the center of the tunnels. At  $400^\circ\text{C}$  the electrical conductivity amounts to  $10^{-3} \Omega^{-1} \text{cm}^{-1}$  with a corresponding activation energy of 0.3 eV, corresponding to the  $\text{Ba}^{2+}$  migration. However, neither ionic nor electronic transference numbers could be determined within these different temperature intervals, and the interpretations are only based on frequency dependent dielectric relaxation data. As found from X-ray diffraction studies<sup>113</sup> and from NMR investigations<sup>115</sup> on other related  $\text{Ba}^{2+}$  priderites, the displacements of the  $\text{Ba}^{2+}$  cations should not be attributed to a long-range migration but rather to a local back and forth motion. Since the nature of the charge carriers is not verified in detail by additional electrical measurements, there still exists a possibility of predominantly electronic conduction in this material, particularly in the high-temperature region, which is caused by charge-transfer processes between Fe and/or Ti ions, without any conductivity contribution due to a divalent cation transport. At this point in the current investigations, the assignment of  $\text{Ba}_x\text{Ti}_{4-2x}\text{Fe}_{2x}\text{O}_8$  ( $x = 0.67$ ) as a divalent cationic conductor does not seem to be justified. Additional research has to be done to investigate its transport properties and to examine whether the measured ionic movements belong to a long-range or a short-range migration.

## 6. Trivalent Cationic Conductors

**6.1.  $\beta$ -Alumina.** *6.1.1.  $\text{M}^{3+}-\beta''$ -Alumina. Single Crystals.* As for divalent cations, a trivalent ion exchange into the conduction planes of  $\text{Na}^+-\beta''\text{-Al}_2\text{O}_3$  crystals is also possible and has been performed for various kinds of cations, including Bi,<sup>43</sup> Cr,<sup>43</sup> La,<sup>116</sup> Pr,<sup>117–119</sup> Nd,<sup>43</sup> Sm,<sup>43</sup> Eu,<sup>43</sup> Gd,<sup>30,120</sup> Tb,<sup>43</sup> Ho,<sup>121,122</sup> Er,<sup>43</sup> and Yb.<sup>43</sup>  $\text{Gd}^{3+}-\beta''\text{-Al}_2\text{O}_3$  was prepared by the usual exchange reaction in 1983<sup>30</sup> and claimed to be the first solid electrolyte conducting trivalent cations.<sup>120</sup> Although  $\text{Gd}^{3+}-\beta''\text{-Al}_2\text{O}_3$  is an insulator at room temperature ( $\sigma_{\text{RT}} < 10^{-11} \Omega^{-1} \text{cm}^{-1}$ ), the conductivity at elevated temperatures increases rapidly and is assumed to result from a  $\text{Gd}^{3+}$  transport, generating a conductivity of  $10^{-3} \Omega^{-1} \text{cm}^{-1}$  at  $600\text{--}700^\circ\text{C}$ .<sup>30,121</sup> For other lanthanide ion ( $\text{Ln} = \text{La}, \text{Pr}, \text{Nd}$ ) exchanged  $\text{Ln}^{3+}-\beta''\text{-Al}_2\text{O}_3$  crystals, conductivity values of  $10^{-4}\text{--}10^{-6} \Omega^{-1} \text{cm}^{-1}$  have been reported for temperatures around  $400\text{--}500^\circ\text{C}$ .<sup>44,116,118</sup>

However, whether this conductivity is really due to the transport of trivalent cations or/and remaining sodium cations,<sup>121</sup> protons, oxygen anions, or electronic charge carrier has not yet been investigated in detail. Critically stated, the observed conduction behavior can also be interpreted by assuming the existence of non-mobile trivalent cations and unexchanged  $\text{Na}^+$  cations which exclusively transport the ionic current, even at high temperatures. Higher activation energies are due to increased repulsive forces experienced by the fixed trivalent cations and lowered conductivities caused by the reduced number of charge carriers. For example,

the composition of ion-exchanged  $\text{Gd}^{3+}\text{-}\beta''\text{-Al}_2\text{O}_3$  crystals has been determined by radiochemical techniques using  $^{22}\text{Na}$  isotopes. During the ion exchange procedures, the  $^{22}\text{Na}$  activity can usually be reduced by 3 orders of magnitude.<sup>28</sup> Thus, about 0.1% of the initial sodium content might remain within the samples. Assuming only  $\text{Na}^+$  cations as mobile charge carriers, the conductivity should also be decreased by at least 3 orders of magnitude. If the conductivity of the  $\text{Gd}^{3+}\text{-}\beta''\text{-Al}_2\text{O}_3$  crystals is higher, it would be a clear indication for additional conductivity contributions by mobile  $\text{Gd}^{3+}$  cations. However, since the conductivity of the unexchanged  $\text{Na}^+\text{-}\beta''\text{-Al}_2\text{O}_3$  crystals is about 4 orders of magnitude higher ( $\sigma_{600-700\text{ }^\circ\text{C}} = 10^1 \Omega^{-1} \text{cm}^{-1}$ ), a  $\text{Gd}^{3+}$  migration cannot be certainly concluded and additional measurements have to be performed in order to clarify this matter. But unfortunately, the trivalent ion exchanged  $\text{M}^{3+}\text{-}\beta''\text{-alumina}$  are not as well characterized by various kinds of experiments, as the corresponding divalent compounds. Only impedance and X-ray measurements are available, which indicate the trivalent cationic current transport. On the other hand, since these compounds are synthesized by ion exchange reactions, there is no doubt about the diffusion properties of the trivalent cations in a chemical concentration gradient. But attempts to connect this diffusion to a migration in an electrical potential gradient, as expressed in the Nernst–Einstein equation, have not been made. For this purpose, it is possible to estimate the diffusion coefficient from the experimental conditions (exchange time, temperature, size of the crystals, etc.) in the corresponding ion exchange experiments. This diffusion coefficient can be used in the Nernst–Einstein equation to calculate a theoretical conductivity value, which should be the same or at least similar to the measured conductivity data at the corresponding temperature. A qualitative agreement between both sets of conductivity data could be observed for  $\text{Gd}^{3+}\text{-}\beta''\text{-Al}_2\text{O}_3$  as well as  $\text{Pr}^{3+}\text{-}\beta''\text{-Al}_2\text{O}_3$  crystals (experimental data are taken from refs 30, 120 and 44, 118, respectively), which indicates a trivalent cationic conduction within these compounds. Although this calculation cannot serve as a direct and quantitative demonstration for the presence of mobile trivalent cationic charge carriers, it gives at least some positive preliminary results until the final verification can be drawn from corresponding appropriate experiments.

Most of the investigations concerning the electrical conduction properties in  $\text{M}^{3+}\text{-}\beta''\text{-Al}_2\text{O}_3$  have been performed by impedance spectroscopic measurements on lanthanide ion exchanged systems. Especially the cation concentration or the  $\text{M}^+/\text{M}^{3+}$  ratio in the conduction planes and its influence on the electrical conductivity is of special interest concerning the identification of mobile trivalent charge carrier. As an example, Figure 8 displays the dependence of the ionic conductivity on the crystal composition (determined by EPMA), i.e., the degree of exchange,  $\xi$ , as measured on  $\text{Na}^+/\text{Pr}^{3+}\text{-}\beta''\text{-Al}_2\text{O}_3$  crystals for two temperatures.<sup>118,119</sup> The different behaviors are interpreted in terms of a  $\text{Pr}^{3+}$  motion; in the low-temperature regime, the conduction is only due to the motion of residual sodium ions, whereas the lanthanide ions remain fixed within their crystallographic positions. Hence, the conductivity sharply

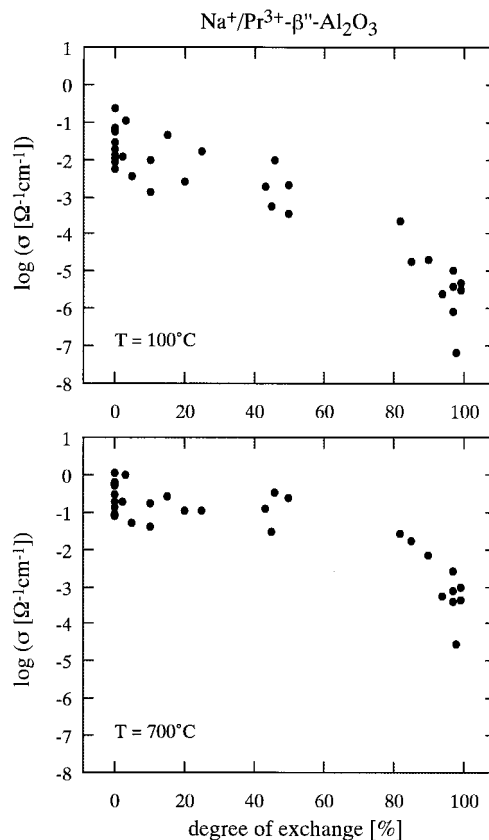


**Figure 8.** Ionic conductivities ( $\log \sigma$ ) of  $\text{Na}^+/\text{Pr}^{3+}\text{-}\beta''\text{-Al}_2\text{O}_3$  crystals as a function of the degree of exchange at 100 °C and 700 °C. Reproduced with permission from ref 118. Copyright 1996 Academic Press.

and continuously decreases with increasing  $\text{Pr}^{3+}$  content due to (i) the reduction in mobile charge carrier concentration, (ii) the raised steric hindrance created by narrowing the conduction slabs, and (iii) the blocking of the pathways by the immobile trivalent cations (cf. Figure 8a). At higher temperatures, the  $\text{Pr}^{3+}$  cations are thermally activated and also become mobile, giving rise to additional conductivity contributions. The  $\sigma$  decrease due to the numerous reduction of monovalent charge carriers is nearly balanced by the increased charge transport of the trivalent cations, and the conductivity remains almost constant ( $\text{Na}^+/\text{Pr}^{3+}\text{-}\beta''\text{-Al}_2\text{O}_3$  with  $10\% < \xi < 50\%$ ). In highly exchanged samples ( $\xi > 50\%$ ) the numerical reduction of charge carriers becomes the deciding factor which cannot be compensated by the comparatively slow moving trivalent cations (cf. Figure 8b). Nevertheless, at high temperatures ( $T > 300\text{ }^\circ\text{C}$ ), all cations within the conduction planes contribute to the observed conductivity.

Other attempts to elucidate to what extent  $\text{Pr}^{3+}$  cations in  $\text{Pr}^{3+}\text{-}\beta''\text{-Al}_2\text{O}_3$  are mobile or not concern the evaluation of X-ray data. The crystal structure of highly exchanged  $\text{Ln}^{3+}\text{-}\beta''\text{-Al}_2\text{O}_3$  ( $\text{Ln}$  = lanthanide) has been investigated.<sup>44,116,124</sup> One common feature in these structure descriptions is the high anisotropic displacement factors of the lanthanide cations in both crystallographic positions of the conduction planes, as is typically exhibited by di- and monovalent cationic conducting  $\text{M}^{n+}\text{-}\beta''\text{-aluminas}$ . Temperature-dependent X-ray investigations on a  $\text{Pr}^{3+}\text{-}\beta''\text{-Al}_2\text{O}_3$  single crystal



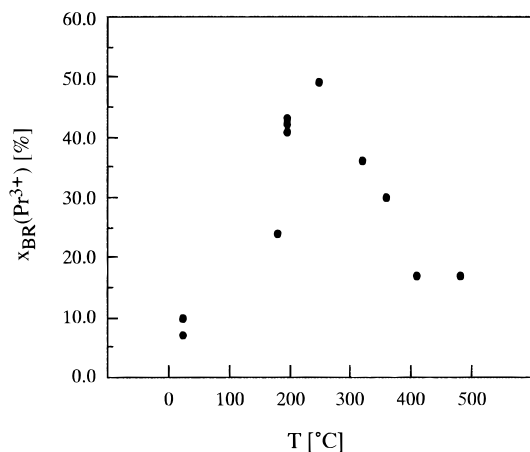


**Figure 9.** Temperature dependence of the relative BR site occupation with Pr<sup>3+</sup> cations ( $x_{BR}(Pr^{3+})$ ) in a Pr<sup>3+</sup>- $\beta''$ -Al<sub>2</sub>O<sub>3</sub> crystal with the composition Na<sub>0.01</sub>Pr<sub>0.53</sub>Mg<sub>0.72</sub>Al<sub>10.33</sub>O<sub>17</sub>. Reproduced with permission from ref 125. Copyright 1997 Wiley-VCH GmbH.

with the composition Na<sub>0.01</sub>Pr<sub>0.53</sub>Mg<sub>0.72</sub>Al<sub>10.33</sub>O<sub>17</sub> give rise to further indications concerning the mobility of the trivalent cations.<sup>125</sup> EPMA analysis was used to determine the composition of the samples, whereas the trivalent oxidation state of the praseodymium cations was established by XANES measurements. The crystal structure, especially the Pr<sup>3+</sup> ion distribution within the available BR and mO sites, was examined at different temperatures in the range between 25 and 500 °C. The results of these measurements are shown in Figure 9 which displays the fractional occupation of the BR site by Pr<sup>3+</sup> cations at different temperatures. At room temperature, about 10% of the lanthanide ions are found in BR positions. With increasing temperature the relative BR occupation rises to a maximum at 250 °C, where both positions (BR and mO sites) are occupied to a nearly equal extent. A further temperature increase causes a redistribution of the main Pr<sup>3+</sup> ion fraction back into the mO sites again.

This behavior indicates a considerable Pr<sup>3+</sup> mobility at increased temperatures. While migrating long distances through the crystal, the mobile cations have to overcome the potential barriers of the nonequivalent BR and mO sites which are distributed along the pathways. Leaving a BR site requires a higher activation energy for the Pr<sup>3+</sup> cations than escaping from a mO position. At comparatively low temperatures ( $T < 250$  °C, cf. Figure 9), the trivalent cations are able to leave the mO sites for adjacent BR positions. However, the further migration out of BR into mO sites is not possible due to an insufficient thermal activation. In consequence, the cationic distribution changes and the Pr<sup>3+</sup> cations accumulate in the BR positions (25 °C  $< T < 250$  °C). At elevated temperatures ( $T > 250$  °C), the thermal activation enables the Pr<sup>3+</sup> cations to migrate out of BR into the next mO positions and the percentage BR occupation decreases (cf. Figure 9). This model is supported by conductivity data which are obtained by impedance spectroscopic measurements on Na<sup>+</sup>/Pr<sup>3+</sup>- $\beta''$ -Al<sub>2</sub>O<sub>3</sub> crystals.<sup>118,119,126</sup> For illustration, the electrical conductivity of Na<sup>+</sup>/Pr<sup>3+</sup>- $\beta''$ -Al<sub>2</sub>O<sub>3</sub> crystals is displayed in Figure 10 for different Pr<sup>3+</sup> concentrations as a function of the temperature. Two temperature regions are distinguishable, giving rise to the following inter-

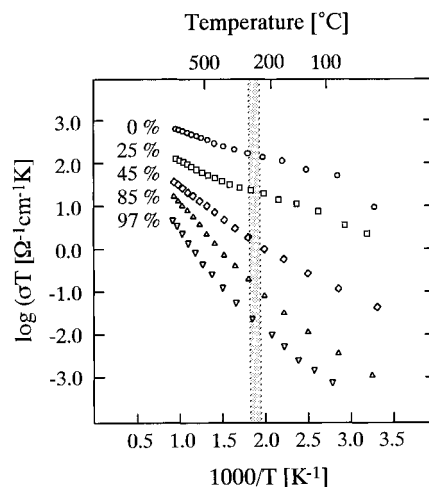


**Figure 10.** Electrical conductivity of Na<sup>+</sup>/Pr<sup>3+</sup>- $\beta''$ -Al<sub>2</sub>O<sub>3</sub> crystals with different degrees of exchange. The shaded region corresponds to the temperature interval where the Pr<sup>3+</sup> cationic motion is assumed to set in. Reproduced with permission from ref 118. Copyright 1996 Academic Press.

pretation. At low temperatures, the conductivity is generated by the mobility of unexchanged Na<sup>+</sup> ions, whereas the ascending curve in the higher temperature range is caused by additional conductivity contributions of mobile Pr<sup>3+</sup> ions. The temperature which can be related to the onset of the Pr<sup>3+</sup> mobility is deduced from the Arrhenius plots to 240 ± 40 °C (by determining the intersection of the two straight lines obtained by the extrapolation of the experimental data within the upper and lower temperature range). This value agrees very well with the temperature at which the migration of the Pr<sup>3+</sup> cations from BR into mO sites becomes energetically possible, as deduced from the above-mentioned X-ray diffraction measurements (cf. Figure 9). For temperatures below 250 °C, the Pr<sup>3+</sup> ions are trapped within the BR position and unable to exhibit long-range migration. The electrical current in this temperature range is only carried by Na<sup>+</sup> ions, which are able to pass through all crystallographic sites. At temperatures above 250 °C, the trivalent cations become able to overcome all potential barriers along the conduction pathways. Consequently, a long-range trivalent cation transport occurs with an increase in ionic conductivity, as shown in Figure 10.

However, although these experimental data can be interpreted in terms of mobile trivalent cationic species, other explanations based on, for example, hydration effects, ion-ion and ion-vacancy correlation, may exist, which also are suitable to explain the observed data without taking into account a trivalent cationic migration process. Since the electrical properties of M<sup>3+</sup>- $\beta''$ -Al<sub>2</sub>O<sub>3</sub> are only based on methods such as impedance spectroscopy or X-ray diffraction, which cannot provide a direct evidence for the charge carriers, further experiments and additional investigations, such as polarization or electromotive force measurements, as well as dc electrolysis, are helpful and necessary to directly verify the trivalent cations as mobile species.

*Polycrystals.* Following the trend as already mentioned for polycrystalline divalent M<sup>2+</sup>- $\beta''$ -aluminas, the ion exchange into polycrystalline Na<sup>+</sup>- $\beta''$ -Al<sub>2</sub>O<sub>3</sub> is much more difficult than for a single crystalline material, in

particular for the case of trivalent cations. Thus, trivalent ion exchange reactions for polycrystalline  $\text{Na}^+/\beta''\text{-Al}_2\text{O}_3$  have been rarely reported, e.g. for the  $\text{Na}^+/\text{Nd}^{3+}/\beta''\text{-Al}_2\text{O}_3$ <sup>72</sup> and the  $\text{Na}^+/\text{Ce}^{3+}/\beta''\text{-Al}_2\text{O}_3$ <sup>76</sup> systems. But electrical conductivity measurements were not performed on these samples. Furthermore, the grains of the latter compound exhibit microcracks due to tensions in the crystal structure which occur when the large lanthanide ions enter the conduction planes. The  $\text{Ce}^{3+}$  distribution was found to be inhomogeneous, i.e., highly concentrated at the outer regions but only poorly concentrated within the centers of the grains. The ion exchange method appears not to be appropriate to produce polycrystalline  $\text{M}^{3+}/\beta''\text{-Al}_2\text{O}_3$  material.

**6.1.2.  $\text{M}^{3+}/\beta\text{-Alumina}$ .** Trivalent cation exchange reactions are difficult to perform for  $\text{Na}^+/\beta\text{-Al}_2\text{O}_3$  single crystals, in contradiction to  $\text{Na}^+/\beta''\text{-Al}_2\text{O}_3$ . The first successful incorporation of a high amount of trivalent lanthanide ions (up to 95%) was reported for  $\text{Na}^+/\text{Ln}^{3+}/\beta\text{-Al}_2\text{O}_3$  (Ln = Pr, Nd, Ho) only a few years ago.<sup>127–129</sup> However, because these compounds are not characterized by electrical measurements, no quantitative statements can be made concerning the trivalent cationic conduction properties. But the ion exchange ability already qualitatively demonstrates the diffusion properties within these compounds. The exchange kinetics are much slower in comparison to the trivalent ion exchange properties in  $\text{Na}^+/\beta''\text{-Al}_2\text{O}_3$  crystals. This reflects the trend which is observed for ion exchange reactions in mono- as well as divalent  $\text{Na}^+/\text{M}^{n+}/\beta\text{-Al}_2\text{O}_3$  materials. For example, nearly 24 h were necessary at a temperature of 800 °C to obtain  $\text{Na}^+/\text{Pr}^{3+}/\beta\text{-Al}_2\text{O}_3$  single crystals with a 90%  $\text{Na}^+$  replacement. The same exchange rate was obtained under identical conditions with  $\text{Na}^+/\beta''\text{-Al}_2\text{O}_3$  crystals within a few minutes.<sup>126</sup>

Trivalent ion exchange reactions for polycrystalline  $\text{Na}^+/\beta\text{-Al}_2\text{O}_3$  are not reported so far. However, this material is accessible by direct synthesis in conventional solid-state reactions.<sup>80,130,131</sup> As a disadvantage, the compounds formed often cannot be obtained as single-phase products. Unreacted starting material remains, or the compounds crystallize in mixed structures consisting of  $\beta$ -alumina and the more densely packed magnetoplumbite-type ( $\text{Ln}_2\text{O}_3 \cdot 12\text{Al}_2\text{O}_3$ , Ln = lanthanide) structures (see section 6.2). Nevertheless, these compounds exhibit poor, but measurable, conductivities which are interpreted to be caused by trivalent  $\text{Ln}^{3+}$  transport. For example, the conductivity of a ceramic  $\text{La}^{3+}/\beta\text{-Al}_2\text{O}_3$  material prepared by direct synthesis is  $6.1 \cdot 10^{-6}$ – $1.6 \cdot 10^{-2} \Omega^{-1} \text{cm}^{-1}$  in the temperature range 450–1000 °C with activation energies of 0.89–1.02 eV.<sup>131</sup> The electronic transference number, as determined by Wagner's polarization method, is less than 0.01 and indicates a predominantly ionic conduction character. From electromotive force measurements using directly synthesized  $\text{La}^{3+}/\beta\text{-Al}_2\text{O}_3$  as solid electrolyte in an oxide concentration cell such as Pt|Ni, NiO| $\text{La}^{3+}/\beta\text{-Al}_2\text{O}_3$ |Fe, FeO|Pt, further strong indications for a trivalent  $\text{La}^{3+}$  migration are given.<sup>130</sup> Although this material is already characterized, the presence of further charge carriers (protons, oxygen anions, impurities) is not certainly excluded and the  $\text{La}^{3+}$  cation as charge carrier not directly determined from corresponding electrolysis experiments.

**6.2.  $\beta\text{-Alumina-Related Phases}$ .** In the previous chapters, the electrical properties have been described for compounds which were prepared by substituting the mobile sodium ions in the  $\text{Na}/\beta/\beta''$ -aluminas. It is also possible to partially or completely replace  $\text{Al}_2\text{O}_3$  within the spinel framework by other oxides, such as  $\text{Ga}_2\text{O}_3$  or  $\text{Fe}_2\text{O}_3$  forming the corresponding isomorphous  $\beta$ - or  $\beta''$ -gallates<sup>132,133</sup> or  $\beta''$ -ferrites,<sup>134</sup> respectively. For multivalent  $\beta''$ -ferrites, no conductivity measurements have been reported. However, the exchange properties are similar to the corresponding  $\beta''$ -alumina compounds, and comparable conductivity data are expected for this group of materials. On the other hand, the  $\beta''$ -ferrites are connected with the problem of electronic conduction due to a possible valence change between  $\text{Fe}^{3+}$  and  $\text{Fe}^{2+}$  cations in the "spinel blocks". The  $\beta/\beta''$ -gallates often exhibit faster ionic conduction characteristics than the corresponding  $\beta/\beta''$ -alumina compounds. Concerning multivalent mobile cations, it is found that in comparison to  $\text{Na}^+/\beta\text{-Al}_2\text{O}_3$  the di- or trivalent ion exchange is much easier for the mixed  $\text{Na}^+/\beta\text{-}(\text{Al}/\text{Ga})_2\text{O}_3(\text{Na}_{1+x}(\text{Al}_{1-y}\text{Ga}_y)_{11}\text{O}_{17+x/2})$  or  $\beta$ -gallate  $\text{Na}^+/\beta\text{-Ga}_2\text{O}_3(\text{Na}_{1+x}\text{Ga}_{11}\text{O}_{17+x/2})$ . For example, by ion exchange reaction in a  $\text{NdCl}_3$ – $\text{NaCl}$  mixture at 650 °C,  $\text{Nd}^{3+}$ -exchanged crystals with the composition  $\text{Na}_{0.77}\text{Nd}_{0.26}\text{Al}_{7.4}\text{Ga}_{3.6}\text{O}_{17.27}$  were obtained after 16 h. Other exchange reactions with trivalent lanthanide ions into  $\beta$ -aluminogallates have been reported, e.g. for  $\text{Ce}^{3+}$ ,  $\text{Nd}^{3+}$ ,  $\text{Eu}^{2+}/\text{Eu}^{3+}$ .<sup>135–137</sup> The faster exchange properties of these gallate compounds are caused by larger  $\text{Ga}^{3+}$  cations [ $r_{\text{Ga}^{3+}} = 0.076$  nm (coordination number CN = 6),  $r_{\text{Al}^{3+}} = 0.0675$  nm and  $r_{\text{Fe}^{3+}} = 0.069$  nm]<sup>138</sup> which are located mainly in tetrahedral sites within the spinel blocks.<sup>135</sup> Some of these crystallographic positions are located nearby the conduction planes and enlarge the spacing between the two adjacent spinel blocks after they have been occupied with larger cations. As a consequence, the steric hindrance for the migrating cations is reduced, causing faster ion exchange characteristics. But in contradiction to the corresponding  $\beta$ -alumina compounds, the gallates do not exhibit the same thermal stability and are not so commonly used for electric applications.

Another group of material which can be derived from the  $\beta$ -sluminas is given by compounds crystallizing in magnetoplumbite-type ( $\text{A}^{2+}\text{B}^{3+}_{12}\text{O}_{19}$ ) structures (MP). These materials can be directly prepared in conventional solid-state reactions at higher temperatures. Figure 11 compares the crystal structures of  $\text{Na}^+/\beta$ -alumina and magnetoplumbite. Like in  $\text{Na}^+/\beta\text{-Al}_2\text{O}_3$ , there exists a mirror plane in magnetoplumbite, separating two adjacent "spinel" blocks and hosting the large A cations. In contradiction to  $\text{Na}^+/\beta$ -alumina, these planes have no oxygen vacancies but are more densely packed. As the number of the vacant sites for mobile charge carriers decreases and the steric hindrance due to the closer packing increases, compounds in the magnetoplumbite structure type exhibit considerably lowered conductivities and higher activation energies (e.g.  $\sigma_{\text{Sr-MP}} = 6.3 \cdot 10^{-9} \Omega^{-1} \text{cm}^{-1}$ ,  $E_a = 1.36$  eV and  $\sigma_{\text{Sr}^{2+}/\beta\text{-alumina}} = 6.3 \cdot 10^{-6} \Omega^{-1} \text{cm}^{-1}$ ,  $E_a = 0.87$  eV at 730 °C, respectively).<sup>92</sup>

Further examples for compounds crystallizing in magnetoplumbite-like structure types are given by  $\text{LnAl}_{11}\text{O}_{18}$  (Ln = La, Ce, Pr, Nd, Sm) and  $\text{LnAl}_{12}\text{O}_{18}\text{N}$

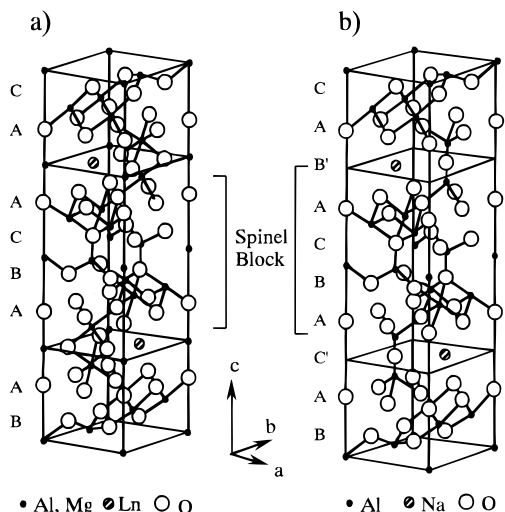


**Figure 11.** Comparison of the hexagonal crystal structures of the magnetoplumbite phase  $\text{LaMgAl}_{11}\text{O}_{19}$  (a) and  $\text{Na}^+\text{-}\beta\text{-Al}_2\text{O}_3$  ( $\text{NaAl}_{11}\text{O}_{17}$ ) (b). Reproduced with permission from Colongues, R.; et al. *J. Solid State Chem.* **1992**, *96*, 97–107. Copyright 1992 Academic Press.

(Ln = La, Ce, Pr, Nd, Sm, Eu, Gd).<sup>139–144</sup> From impedance spectroscopic and EMF measurements, these polycrystalline materials are assumed to conduct trivalent lanthanide cations, generating conductivities of  $3.0 \cdot 10^{-5} \Omega^{-1} \text{ cm}^{-1}$  ( $\text{LaAl}_{11}\text{O}_{18}$ ) and  $8.0 \cdot 10^{-7} \Omega^{-1} \text{ cm}^{-1}$  ( $\text{LaAl}_{12}\text{O}_{18}\text{N}$ ) at  $1000^\circ\text{C}$  and corresponding activation energies of 2.5 and 1.6 eV, respectively.<sup>142,143</sup> But similar to the trivalent  $\text{M}^{3+}\text{-}\beta''\text{-Al}_2\text{O}_3$ , a direct demonstration that this conductivity is purely generated by migrating  $\text{La}^{3+}$  cations is not given, and the possibility of oxygen anionic motion or protons cannot be excluded. On the other hand,  $\text{LaAl}_{12}\text{O}_{18}\text{N}$  ceramics are already tested as high-temperature solid electrolytes and as sensor material for nitrogen.<sup>143</sup> Thus, besides the ion-exchanged  $\text{La}^{3+}\text{-}\beta''\text{-Al}_2\text{O}_3$  and directly synthesized  $\text{La}^{3+}\text{-}\beta\text{-Al}_2\text{O}_3$ , these lanthanum aluminates represent another material in which the ionic current is probably transported by trivalent cations.

**6.3.  $\beta\text{-LaNb}_3\text{O}_9$ .** Besides the family of  $\beta$ -alumina and its related phases, there exist two other different kind of materials for which a trivalent cationic conduction has been claimed. One is given for compounds in the  $\text{Sc}_2(\text{WO}_4)_3$  structure type and will be discussed in the subsequent section. The other one concerns the perovskite-type lanthanum niobate  $\beta\text{-LaNb}_3\text{O}_9$  phase.  $\beta\text{-LaNb}_3\text{O}_9$  is a highly A-cation-deficient perovskite ( $\text{ABO}_3$ ) in a tetragonal crystal structure which is also adopted from the homologous compounds  $\text{Ln}_{1/3}\text{NbO}_3$  with Ln = Ce, Pr, Nd. The corresponding structure type is displayed in Figure 12. Niobium occupies oxygen octahedra sharing common corners in three dimensions. The  $\text{La}^{3+}$  ions are located within the 12-coordinated sites adopting an ordered distribution: parallel to the  $c$ -axis one site is entirely empty and one is statistically occupied by two-thirds of the lanthanum ions.<sup>145</sup> The vacant A positions are energetically equivalent and double the number of total  $\text{La}^{3+}$  ions in the lattice, therefore providing an interconnected 3D-channel for the assumed ionic motion. The electrical conductivity in  $\beta\text{-LaNb}_3\text{O}_9$  is of mixed ionic–electronic nature; at higher temperatures ( $T > 580^\circ\text{C}$ ) the conductivity is

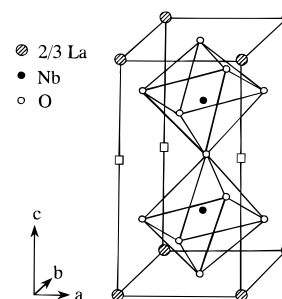


**Figure 12.** Schematic view of the  $\text{LaNb}_3\text{O}_9$  crystal structure.  $\text{La}^{3+}$  vacancies are indicated by  $\square$ . Reproduced with permission from Latie, L.; et al. *J. Solid State Chem.* **1984**, *51*, 293–299. Copyright 1984 Academic Press.

mostly electronic, arising by the formation of ionized oxygen vacancies due to the loss of oxygen (n-type conductor), while in the low-temperature range the conductivity is predominantly ionic ( $\sigma_{400^\circ\text{C}} = 9.9 \cdot 10^{-8} \Omega^{-1} \text{ cm}^{-1}$ ).<sup>146</sup> The ionic transport number is calculated from EMF experiments in the cell  $\text{Pt}(P_{\text{O}_2}) | \text{LaNb}_3\text{O}_9 | (P^*_{\text{O}_2})\text{-Pt}$  ( $P_{\text{O}_2}$  and  $P^*_{\text{O}_2}$  denote different oxygen partial pressures) as well as from polarization measurements. However, the EMF experiment could not be performed at lower temperatures ( $T < 530^\circ\text{C}$ ) even in that temperature region, where a main ionic conduction process is assumed to occur. To characterize the ionic character of the electrical conduction more precisely, an electrolysis experiment was performed using ion-blocking Pt electrodes. After the electrolysis, a difference of the La concentration between the cathodic and anionic surface of the sample was detected. However, the compounds which have been formed were not identified, and a cross-sectional analysis over the whole electrolyzed sample was not given either. The observation of an increased  $\text{La}^{3+}$  concentration at the cathodic surface can also be interpreted in terms of an electrolytic decomposition reactions. Furthermore, temperatures of about  $730^\circ\text{C}$  have been applied for the electrolysis. But for this temperature region, a nearly exclusively electronic conduction with an electronic transference number of about 0.95 was observed. Estimating the nature of an ionic charge carrier at temperatures where electronic motion is predominant leads to uncertainty. To unambiguously verify the trivalent cationic motion in  $\beta\text{-LaNb}_3\text{O}_9$ , the ionic transference number should be determined by a dc electrolysis within the Tubandt setup at temperatures where a main ionic conduction is expected. From the given results,  $\text{La}^{3+}$  cations may be mobile in  $\beta\text{-LaNb}_3\text{O}_9$ , as indicated by the electrolysis experiments, but a final and convincing verification cannot be certainly deduced. Although this compound provides the structural conditions for multivalent cationic conduction (e.g. open layers/tunnels, highly charged cations in the host lattice), the poor conductivity data at lower temperatures in addition to the increased electronic conduction at higher temperatures are serious disadvantages which diminish its potential use in technical application as a solid electrolyte.

**6.4.  $\text{Sc}_2(\text{WO}_4)_3$  Structure Type Phases.** Recently, the  $\text{Sc}_2(\text{WO}_4)_3$  structure type phases have gained high interest from a fundamental point of view, even for the purpose of qualitatively and quantitatively demonstrating the trivalent cationic conduction phenomenon in solids. These compounds are clearly found to conduct

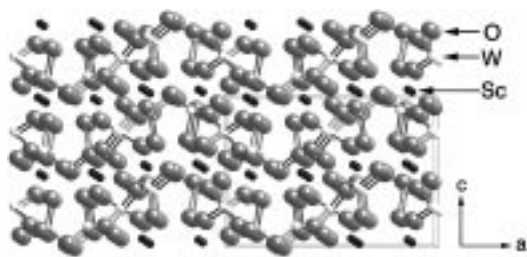


**Figure 13.** Perspective view of the  $\text{Sc}_2(\text{WO}_4)_3$ -type structure along  $[010]$ .

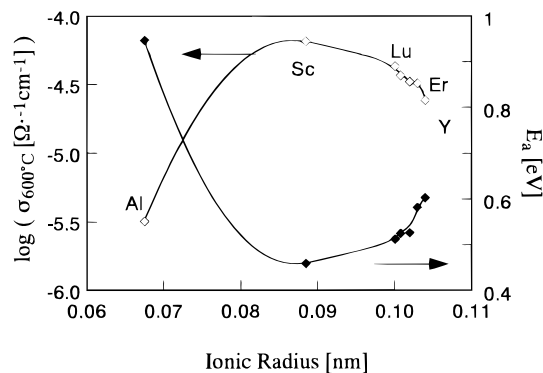


**Figure 14.** The trivalent ionic radius dependencies of the ( $\diamond$ ) electrical conductivity at 600 °C ( $\log(\sigma_{600^\circ\text{C}})$ ) and the ( $\blacklozenge$ ) activation energy  $E_a$  for the trivalent tungstates,  $\text{M}_2(\text{WO}_4)_3$ .

trivalent cations. The orthorhombic  $\text{Sc}_2(\text{WO}_4)_3$  structure type (space group  $Pbcn$ ) is adopted by the tungstates of aluminum, indium, and the smaller lanthanide cations.<sup>147</sup> It consists of a three-dimensional skeleton framework of  $\text{WO}_4$  tetrahedra and  $\text{MO}_6$  octahedra which are linked by corner sharing, as shown in Figure 13. Each octahedron is connected to six tetrahedra, while four octahedra are bonded to one tetrahedron.<sup>148,149</sup> This structure is closely related to that of the high lithium ion conducting compound  $\text{Li}_3\text{Sc}_2(\text{PO}_4)_3$ .<sup>150</sup> Furthermore, a similar building principle consisting of corner-linked octahedra and tetrahedra is realized in the above-mentioned NASICON-type structure.<sup>97,98</sup> As for these superionic conducting compounds, there exist large-sized tunnels in the  $\text{Sc}_2(\text{WO}_4)_3$  structure type in which the cationic migration occurs. Generally, the conductivity in the  $\text{Sc}_2(\text{WO}_4)_3$ -type phases shows anisotropic characteristics with mainly two-dimensional conduction within the  $ab$ -planes (cf. Figure 13).

Preliminary investigations concerning the electrical properties of lanthanide tungstates in the  $\text{Sc}_2(\text{WO}_4)_3$  structure type revealed that these compounds are insulators at room temperature with conductivities less than  $10^{-10} \Omega^{-1} \text{cm}^{-1}$ .<sup>151,152</sup> At elevated temperatures, they become fairly good conductors with typical conductivities of around  $10^{-5}$ – $10^{-6} \Omega^{-1} \text{cm}^{-1}$  ( $T = 600^\circ\text{C}$ ) and corresponding activation energies of 0.41–0.95 eV, depending on the size of the trivalent cation, as shown in Figure 14.<sup>153</sup> The lowest conductivity ( $\sigma_{600^\circ\text{C}} = 3.2 \cdot 10^{-6} \Omega^{-1} \text{cm}^{-1}$ ) and highest activation energy (0.95 eV) among the tungstates is exhibited by  $\text{Al}_2(\text{WO}_4)_3$ , containing the smallest trivalent cation, due to its high charge density and low polarizability. The increase of the cationic size results in enhanced conductivities up to a maximum value for  $\text{Sc}_2(\text{WO}_4)_3$  ( $\sigma_{600^\circ\text{C}} = 6.5 \cdot 10^{-5} \Omega^{-1} \text{cm}^{-1}$ ) combined with a minimum in activation energy (0.46 eV).<sup>151</sup> As the ionic size of the lanthanide cation

increases further, the conductivity decreases again, caused by the enhanced steric hindrance for the ionic motion. Similar dependencies are also found for lanthanide molybdates which crystallize in the  $\text{Sc}_2(\text{WO}_4)_3$ -type structure. For a given cation, the molybdate material always represents the better ion conducting material in comparison to the corresponding tungstates. However, the thermal instability of the molybdates prevent these materials from being used in technical applications where elevated temperatures ( $T > 800$ – $900^\circ\text{C}$ ) are needed to achieve reasonable conductivities.

In the mixed tungstates of the type  $(\text{Sc}_{1-x}\text{M}_x)_2(\text{WO}_4)_3$  ( $\text{M} = \text{Al}, \text{Lu}, \text{Gd}$ ), the conductivity always shows complex behavior, depending on the concentration and size of the substituting cation. Scandium substitution by aluminum cations leads to a decrease in ionic conductivity in comparison to pure  $\text{Sc}_2(\text{WO}_4)_3$ . On the other hand, the conducting properties can be improved by the incorporation of the larger cations  $\text{Gd}^{3+}$  and  $\text{Lu}^{3+}$ , for example in  $\text{Sc}_{1.6}\text{Gd}_{0.4}(\text{WO}_4)_3$ , which exhibits the highest conductivity ( $\sigma_{600^\circ\text{C}} = 6.2 \cdot 10^{-5} \Omega^{-1} \text{cm}^{-1}$ ) among the tungstate solid solutions in the  $\text{Sc}_2(\text{WO}_4)_3$  structure type.<sup>153</sup> This increase is caused by an isotropic expansion of the crystal lattice, leading to widened conduction tunnels, which in turn allows an easier cationic migration.

Several different kinds of electric methods including polarization and EMF measurements as well as dc electrolysis experiments have been used to characterize the electrical properties for these compounds, such as  $\text{M}_2(\text{WO}_4)_3$  ( $\text{M} = \text{Al}, \text{Sc}, \text{Y}, \text{Er}$ )<sup>12,154,155</sup> and  $\text{Al}_2(\text{WO}_4)_3$ - $x\text{Al}_2\text{O}_3$ .<sup>156</sup> All these compounds show a clear time-dependent polarization behavior in dc polarization measurements. The dc conductivity abruptly decreases and approaches a steady-state value in a given time interval after applying a small electrical potential gradient (as already shown in Figure 1). The polarization of the sample results from the migration of cationic species to the cathode, and the ionic transference number was determined to be higher than 99% (in the pure tungstates) and 95% (in the composite material), respectively. Furthermore, the anionic oxygen migration can also be excluded from these measurements, since the polarization behavior was found to be the same in different atmospheres varying in oxygen partial pressure. Special dc electrolysis experiments have been used to identify and characterize the trivalent cationic charge carriers. For example, two different tungstate samples are used as solid electrolytes in the cell  $\text{Pt}_{\text{anode}} | \text{Al}_2(\text{WO}_4)_3 | \text{Sc}_2(\text{WO}_4)_3 | \text{Pt}_{\text{cathode}}$ , as shown in Figure 15. After the electrolysis, spot-like deposits were formed on the cathodic surface of the  $\text{Sc}_2(\text{WO}_4)_3$  pellet. EPMA analysis revealed a homogeneous  $\text{Al}^{3+}$  content over the entire cross section of the  $\text{Sc}_2(\text{WO}_4)_3$  sample and precipitation of  $\text{Al}_2\text{O}_3$  and  $\text{Sc}_6\text{WO}_{12}$  on the cathodic surface. These observations lead to the conclusion that  $\text{Al}^{3+}$  cations migrate during the electrolysis out of the  $\text{Al}_2(\text{WO}_4)_3$  through the  $\text{Sc}_2(\text{WO}_4)_3$  phase and precipitate on the cathodic side as  $\text{Al}_2\text{O}_3$ .  $\text{Sc}^{3+}$  cations are also mobile in  $\text{Sc}_2(\text{WO}_4)_3$  and chemically react after reaching the cathodic surface by forming  $\text{Sc}_6\text{WO}_{12}$  deposits.<sup>157</sup>

The quantitative confirmation of the aluminum mobility in  $\text{Al}_2(\text{WO}_4)_3$  was drawn from EMF measurements using different aluminum–platinum alloys in the electric cells  $\text{Al}_{55}\text{Pt}_{45} | \text{Al}_2(\text{WO}_4)_3 | \text{Al} - \text{Pt}$  ( $\text{Al} - \text{Pt}$  represents

**Table 3. Comparison of the Experimental Methods Which Have Been Applied (x) or Not (-), to Characterize the Compounds for Which a Multivalent Cationic Conduction Is Assumed<sup>a</sup>**

ionic conducting compd	impedance	polarization	conductivity or polarization in diff atm	EMF	dc electrolysis + detailed analysis	tubandt or related electrolysis	refs
Divalent Cationic Conductors							
CaS	x	-	x	x	-	x	20–25
M <sup>2+</sup> -β''-alumina (IE)	x	x	-	x	-	-	28, 49, 52, 53, 75
M <sup>2+</sup> -β''-alumina (DS)	x	x	-	x	-	-	68, 79, 80
M <sup>2+</sup> -β-alumina (IE)	x	-	-	-	-	-	84
M <sup>2+</sup> -β-alumina (DS)	x	x	-	x	-	-	91–96
M <sup>2+</sup> Zr <sub>4</sub> (PO <sub>4</sub> ) <sub>6</sub>	x	x	-	-	x	x	99–101, 105
YPO <sub>4</sub> -based compds	x	-	-	x	x	x	110
Ba <sub>x</sub> Ti <sub>4-2x</sub> Fe <sub>2x</sub> O <sub>8</sub> (hollandite)	x	-	-	-	-	-	114
Trivalent Cationic Conductors							
M <sup>3+</sup> -β''-alumina (IE)	x	-	-	-	-	-	46, 118, 123, 125
M <sup>3+</sup> -β-alumina (DS)	x	x	-	x	-	-	130, 131
β-alumina-related phases	x	-	-	x	-	-	139, 141–143
β-LaNb <sub>3</sub> O <sub>9</sub>	x	x	x	x	-	-	146
Sc <sub>2</sub> (WO <sub>4</sub> ) <sub>3</sub> -type phases	x	x	x	x	x	x	12, 153–157

<sup>a</sup> β-Alumina compounds which are prepared by ion exchange or by direct synthesis are denoted by (IE) and (DS), respectively. Further information about the experimental methods is given in the text. Some representative references are given in addition.

Al<sub>55</sub>Pt<sub>45</sub>, Al<sub>42</sub>Pt<sub>58</sub>, and Al<sub>35</sub>Pt<sub>65</sub> alloys, respectively). The electromotive force measured for Al<sub>2</sub>(WO<sub>4</sub>)<sub>3</sub> in these cells agrees very well with theoretical calculations, and the ionic transference number could be quantitatively determined to be unity.<sup>13</sup>

Combining these experimental results, the conclusion can be drawn that the tungstate compounds in the Sc<sub>2</sub>(WO<sub>4</sub>)<sub>3</sub>-type structure are trivalent cation conducting solid electrolytes where the mobility of the trivalent cationic charge carriers has been directly and undoubtedly demonstrated.

## 7. Evidence for Multivalent Cationic Conduction

In the previous sections, materials are presented for which a multivalent ( $n \geq 2$ ) cationic conduction is reported to occur. The electrical properties and even the charge carriers are characterized by various electrochemical methods. Table 3 gives a brief summary about the experiments which have been performed on these materials and from which the assumptions for a multivalent cationic current transport are extracted. The most convincing and unambiguous demonstration of ionic and multivalent cationic conduction is given by Tubandt or related electrolysis experiments. But referring to Table 3, only a few compounds have been characterized by this method, namely CaS, M<sup>2+</sup>Zr<sub>4</sub>(PO<sub>4</sub>)<sub>6</sub>, divalent YPO<sub>4</sub>-based compounds and tungstates in the Sc<sub>2</sub>(WO<sub>4</sub>)<sub>3</sub>-type structure. The possibility of diffusion in M<sup>n+</sup>-β''-Al<sub>2</sub>O<sub>3</sub> has already been shown by the ion exchange reactions. However, the direct and final verification for the migrating M<sup>n+</sup> cations by electrolysis experiments is still lacking. Divalent M<sup>2+</sup>-β''-Al<sub>2</sub>O<sub>3</sub> are electrically well-characterized by a various number of distinct experiments including, for example, the examination of transference numbers and a qualitative demonstration of the divalent cationic migration properties. A corresponding thorough investigation is not available for trivalent M<sup>3+</sup>-β''-Al<sub>2</sub>O<sub>3</sub>, although these compounds are commonly accepted as trivalent cation conducting compounds. But besides the ionic exchange

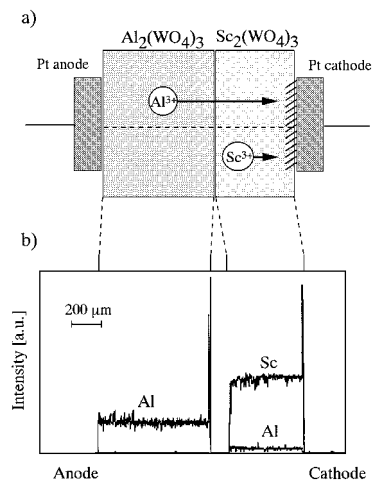


**Figure 15.** (a) Schematic view of the electrolysis cell for Al<sub>2</sub>(WO<sub>4</sub>)<sub>3</sub>/Sc<sub>2</sub>(WO<sub>4</sub>)<sub>3</sub>. The hatched region indicates the area of Al<sub>2</sub>O<sub>3</sub> and Sc<sub>6</sub>WO<sub>12</sub> deposits, whereas the dotted line represents a cross line section for the EPMA analysis as shown in part b). (b) Cross sectional EPMA line analysis for the corresponding Al<sub>2</sub>(WO<sub>4</sub>)<sub>3</sub> and Sc<sub>2</sub>(WO<sub>4</sub>)<sub>3</sub> pellets after the electrolysis.

reactions, impedance spectroscopic, and XRD measurements, no further efforts have been reported to directly identify the trivalent species as mobile charge carriers in M<sup>3+</sup>-β''-Al<sub>2</sub>O<sub>3</sub>.

For other compounds which have not been prepared by ion exchange reaction, the mutual combination of several different experiments and measurements is of high importance and absolutely necessary, since the qualitative demonstration of the cationic mobility is not available from the diffusive ion substitution. For some of these materials, it can be stated that the multivalent ( $n \geq 2$ ) cationic migration process is not sufficiently and precisely characterized. In these cases, doubts remain concerning the interpretation whether the observed conductivity is really due to the migration of mobile di- or trivalent cations. This conclusion does not mean that these compounds are not cationic conductors at all. However, the results of the performed experiments

cannot serve as direct evidence but only give indications of a more or less conclusive extent.

### 8. Conclusions

Multivalent cationic conduction in solids is still a developing field in electrochemistry, especially with regard to charge carriers in an oxidation state higher than two. But from the presented results it can be argued that there is no doubt about the fundamental possibility of multivalent cationic migration. However, caution and the appropriate combination of experimental techniques need to be applied before definite conclusions of multivalent conduction can be drawn. Further research has to be done for some materials in which mobile multivalent cations are expected to occur, to establish this phenomenon more thoroughly and precisely.

For the purpose of clarifying the nature of a charge carrier in detail, dc electrolysis techniques, especially the Tubandt electrolysis, should be used in which the migration of the mobile cationic species can be observed macroscopically. In addition, the possibility for the presence or absence of other charge carriers, like e.g. protons, anions, or electrons/holes, has to be examined in detail by the corresponding experimental methods. Only the combination of these different methods reliably leads to the exclusion of all doubts concerning the multivalent cationic ( $n \geq 2$ ) current transport.

Besides basic research regarding the characteristics of multivalent cationic conduction, the investigation of the corresponding materials used as solid electrolytes in technical applications is a further interesting and challenging task, even with regard to some already known successful applications concerning thermodynamical studies or sensor devices. Soon, the phenomenon of a multivalent cationic conduction in solids, in particular with mobile cationic charge carriers in an oxidation state higher than two, should be established more thoroughly.

**Acknowledgment.** The present work was partially supported by a Grant-in-Aid for Scientific Research No. 09215223 on Priority Areas (No. 260), Nos. 06241106, 06241107, and 093065 from The Ministry of Education, Science, Sports and Culture. It was also supported by the "Research for the Future, Preparation and Application of Newly Designed Solid Electrolytes (JSPS-RFTF96P00102)" program from the Japan Society for the Promotion of Science (JSPS). J. Köhler gratefully acknowledges his postdoctoral fellowship for foreign researchers in Japan from the JSPS.

### References

- "I must point out that the authors have not by any means demonstrated that their compound conducts  $Al^{3+}$  ions. Extraordinary claims require extraordinary proof, and they have made the former but not the latter." This paragraph is part of a reviewer's comment about a paper which dealt with the identification of trivalent  $Al^{3+}$  conduction in solids and which was submitted by the authors of this article (N. Imanaka and G. Adachi) for publication in a high-ranking scientific journal in January 1997.
- Tubandt, C. *Handbuch der Experimentellen Physik*; Springer-Verlag: Berlin, 1932; Bd XII.
- Réau, J. M.; Portier, J.; Levasseur, A. *Mater. Res. Bull.* **1978**, *13*, 1415.
- West, A. R. *Solid State Chemistry and its Applications*; Wiley & Sons: New York, 1984.
- Nomura, K.; Ikeda, S.; Ito, K.; Einaga, H. *Solid State Ionics* **1993**, *61*, 29.
- Wagner, C. *Proc. Intern. Comm. Electrochem. Thermodyn. Kinet.* **1957**, *7*, 361.
- Gellings, P. J.; Bouwmeester, H. J. M. *The CRC Handbook of Solid State Electrochemistry*; CRC Press: Boca Raton, 1997.
- Kudo, T.; Fueki, K. *Solid State Ionics*; VCH Verlag: Weinheim, 1990.
- Bauerle, J. E. *J. Phys. Chem. Solids* **1969**, *30*, 2657.
- Macdonald, J. R. *Impedance Spectroscopy*; Wiley & Sons: New York, 1987.
- Archer, W. I.; Armstrong, R. D. *Electrochem.* **1989**, *7*, 157.
- Wagner, C. *Z. Electrochem.* **1956**, *60*, 4.
- Kobayashi, Y.; Egawa, T.; Tamura, S.; Imanaka, N.; Adachi, G. *Chem. Mater.* **1997**, *9*, 1649.
- Johansen, H. A.; Cleary, J. G. *J. Electrochem. Soc.* **1964**, *111*, 100.
- Tubandt, C. *Z. Anorg. Allg. Chem.* **1921**, *115*, 105.
- Tubandt, C.; Reinhold, H. *Z. Electrochem.* **1923**, *29*, 313.
- Schwab, G. M.; Eulitz, G. *Z. Phys. Chem.* **1967**, *55*, 179.
- Seguchi, Y.; Mekata, M. *J. Phys. Soc. Jpn.* **1985**, *54*, 3447.
- Ukyo, Y.; Goto, K. S.; Inomata, Y. *J. Am. Ceram. Soc.* **1978**, *62*, 410.
- Worrell, W. L.; Tare, V. B.; Bruni, F. *J. High-temperature technology*; Butterworth: London, 1969; p 503.
- Wen, T. L.; Weppner, W.; Rabenau, A. *Z. Anorg. Allg. Chem.* **1983**, *497*, 93.
- Sato, M.; Imanaka, N.; Adachi, G.; Shiokawa, J. *Mater. Res. Bull.* **1981**, *16*, 215.
- Adachi, G.; Imanaka, N.; Sato, M.; Shiokawa, J. *Bull. Chem. Soc. Jpn.* **1985**, *58*, 550.
- Egami, A.; Onoye, T.; Narita, K. *Solid State Ionics* **1981**, *3/4*, 617.
- Nagata, K.; Goto, K. S. *Metall. Trans.* **1974**, *5*, 899.
- Yao, Y.-F. Y.; Kummer, J. T. *J. Inorg. Nucl. Chem.* **1967**, *29*, 2453.
- Dunn, B.; Farrington, G. C. *Mater. Res. Bull.* **1980**, *15*, 1773.
- Farrington, G. C.; Dunn, B. *Solid State Ionics* **1982**, *7*, 267.
- Tokopov, N. A.; Stukalova, M. M. *C. R. Akad. Sci. SSSR* **1940**, *27*, 974.
- Dunn, B.; Farrington, G. C. *Solid State Ionics* **1983**, *9/10*, 223.
- Banks, E.; Ward, R. *J. Electrochem. Soc.* **1949**, *96*, 297.
- Yakel, H. L.; Banks, E.; Ward, R. *J. Electrochem. Soc.* **1949**, *96*, 304.
- Beevers, C. A.; Ross, M. A. *Z. Kristallogr.* **1937**, *97*, 59.
- Bettman, M.; Peters, C. R. *J. Phys. Chem.* **1969**, *73*, 1774.
- Whittingham, M. S.; Huggins, R. A. *J. Chem. Phys.* **1971**, *54*, 414.
- Collongues, R.; Gourier, D.; Kahn, A.; Boilot, J. P.; Colombari, Ph.; Wicker, A. *J. Phys. Chem. Solids* **1984**, *45*, 981.
- Engstrom, H.; Bates, J. B.; Brundage, W. E.; Wang, J. C. *Solid State Ionics* **1981**, *2*, 265.
- Saalfeld, H.; Matthies, H.; Datta, S. K. *Ber. Deutsch. Keram. Ges.* **1968**, *45*, 212.
- Radzilowski, R. H.; Kummer, J. T. *Inorg. Chem.* **1969**, *8*, 2531.
- Kummer, J. T. *Prog. Solid State Chem.* **1972**, *7*, 141.
- Radzilowski, R. H. *Inorg. Chem.* **1969**, *8*, 994.
- Dedecke, T.; Köhler, J.; Tietz, F.; Urland, W. *Eur. J. Solid State Inorg. Chem.* **1996**, *33*, 185.
- Sattar, S.; Ghosal, B.; Underwood, M. L.; Mertwoy, H.; Saltzberg, M. A.; Frydrych, W. S.; Rohrer, G. S.; Farrington, G. C. *J. Solid State Chem.* **1986**, *65*, 231.
- Köhler, J.; Urland, W. *J. Solid State Chem.* **1996**, *124*, 169.
- Fowles, E. H.; Labinger, J. A.; Beauchamp, J. L.; Fultz, B. *J. Phys. Chem.* **1991**, *95*, 7393.
- Dunn, B.; Farrington, G. C.; Thomas, J. O. *MRS Bull.* **1989**, *14*, 22.
- The termination "complete ion exchange" is somewhat confusing. Complete ion exchange indicates a sodium replacement to 100%. But this is not possible in practice due to statistical reasons. However, the  $Na^+$  activity can be reduced by at least 3 orders of magnitude and its concentration becomes comparable to the impurity concentration in available reagents. Such a replacement can be considered as a "complete exchange" since it is as complete as possible. Nevertheless, this point of uncertainty should be kept in mind when considering the interpretation of conductivity data in ion-exchanged samples. Highly ion-exchanged compounds referring to the chemical formula  $M^{n+}\beta^-Al_2O_3$  always contain a small amount of  $Na^+$  ions. See also ref 121.
- Ni, J.; Tsai, Y. T.; Whitmore, D. H. *Solid State Ionics* **1981**, *5*, 199.
- SeEVERS, R.; DeNuzzio, J.; Farrington, G. C.; Dunn, B. *J. Solid State Ionics* **1983**, *50*, 146.
- Dunn, B.; Ostrom, R. M.; SeEVERS, R.; Farrington, G. C. *Solid State Ionics* **1981**, *5*, 203.
- Lane, C.; Farrington, G. C.; Thomas, J. O.; Zendejas, M. A. *Solid State Ionics* **1990**, *40/41*, 53.
- Rohrer, G. S.; Thomas, J. O.; Farrington, G. C. *Chem. Mater.* **1990**, *2*, 395.

- (53) Rohrer, G. S.; Farrington, G. C. *J. Solid State Chem.* **1990**, *85*, 299.
- (54) Rohrer, G. S.; Davies, P. K.; Farrington, G. C. *Solid State Ionics* **1988**, *28-30*, 354.
- (55) Carrillo-Cabrera, W.; Thomas, J. O.; Farrington, G. C. *Solid State Ionics* **1985**, *17*, 223.
- (56) Barrie, J. D.; Dunn, B.; Stafuss, O. M.; Farrington, G. C. *Solid State Ionics* **1986**, *18/19*, 677.
- (57) Park, S. M.; Hellstrom, E. E. *Solid State Ionics* **1990**, *44*, 55.
- (58) Ghosal, B.; Mangle, E. A.; Topp, M. R.; Dunn, B.; Farrington, G. C. *Solid State Ionics* **1983**, *9/10*, 273.
- (59) Saltzberg, M. A.; Garzon, F. H.; Davies, P. K.; Farrington, G. C. *Solid State Ionics* **1988**, *28/30*, 386.
- (60) Saltzberg, M. A.; Thomas, J. O.; Farrington, G. C. *Chem. Mater.* **1989**, *1*, 19.
- (61) Pechenik, A.; Whitmore, D. H.; Ratner, M. A. *J. Chem. Phys.* **1986**, *84*, 2827.
- (62) Pechenik, A.; Whitmore, D. H.; Ratner, M. A. *Solid State Ionics* **1983**, *9/10*, 287.
- (63) Dunn, B.; Farrington, G. C. *Solid State Ionics* **1986**, *18/19*, 31.
- (64) Breiter, M. W.; Maly-Schreiber, M.; Allitsch, G.; Linhardt, P. *Solid State Ionics* **1988**, *28/30*, 369.
- (65) Hellstrom, E. E.; Benner, R. E. *Solid State Ionics* **1983**, *11*, 125.
- (66) Whiter, J. T.; Fray, D. J. *Solid State Ionics* **1985**, *17*, 1.
- (67) Sammells, A. F.; Schumacher, B. *J. Electrochem. Soc.* **1986**, *133*, 235.
- (68) Hong, Y.; Hong, D.; Peng, Y.; Li, L.; Wei, S. *Solid State Ionics* **1987**, *25*, 301.
- (69) Franceschetti, D. R.; Hellstrom, E. E. *Solid State Ionics* **1988**, *28/30*, 381.
- (70) Allitsch, G.; Linhardt, P.; Breiter, M. W. *Solid State Ionics* **1989**, *31*, 313.
- (71) Schaefer, G. W.; Weppner, W. *Solid State Ionics* **1992**, *53/56*, 559.
- (72) Yang, D. L.; Dunn, B.; Morgan, P. E. D. *J. Mater. Sci. Lett.* **1991**, *10*, 485.
- (73) Maly-Schreiber, M.; Linhardt, P.; Breiter, M. W. *Electrochim. Acta* **1987**, *32*, 1371.
- (74) Rög, G.; Kozłowska-Rög, A. *Electrochim. Acta* **1985**, *30*, 335.
- (75) Rög, G.; Pycior, W.; Kozłowska-Rög, A. *Solid State Ionics* **1988**, *28/30*, 391.
- (76) Wen, Z. Y.; Lin, Z. X.; Tian, S. B. *Solid State Ionics* **1990**, *40/41*, 91.
- (77) Wen, Z. Y.; Lin, Z. X.; Tian, S. B. *J. Chin. Inorg. Mater.* **1987**, *2*, 239.
- (78) Crosbie, G. M.; Tennenhouse, G. J. *J. Am. Ceram. Soc.* **1982**, *65*, 187.
- (79) Kumar, R. V.; Kay, D. A. R. *Metall. Trans. B* **1985**, *16*, 107.
- (80) Kumar, R. V.; Kay, D. A. R. *Metall. Trans. B* **1985**, *16*, 295.
- (81) Whittingham, M. S.; Huggins, R. A. *J. Chem. Phys.* **1971**, *54*, 414.
- (82) Edstroem, K.; Thomas, J. O.; Farrington, G. C. *Acta Crystallogr. B* **1991**, *47*, 635.
- (83) Zendejas, M. A.; Thomas, J. O. *Phys. Scr.* **1990**, *T33*, 235.
- (84) Sutter, P. H.; Cratty, L.; Saltzberg, M.; Farrington, G. C. *Solid State Ionics* **1983**, *9/10*, 295.
- (85) Boilot, J. P.; Colomban, Ph.; Lee, M. R.; Collin, G.; Comes, R. *Solid State Ionics* **1983**, *9/10*, 315.
- (86) Catti, M.; Cazzanelli, E.; Ivaldi, G.; Mariotto, G. *Phys. Rev. B* **1987**, *36*, 9451.
- (87) McWhan, D. B.; Dernier, P. D.; Vettier, C.; Cooper, A. S.; Remeika, J. P. *Phys. Rev. B* **1978**, *17*, 4043.
- (88) Staikov, G.; Nikolov, V.; Yankulov, P. D. *Solid State Ionics* **1988**, *28/30*, 373.
- (89) Flinn, D. R.; Stern, K. H. *J. Electrochem. Soc.* **1978**, *123*, 978.
- (90) Roumieu, R.; Pelton, A. D. *J. Electrochem. Soc.* **1981**, *128*, 50.
- (91) Rög, G.; Borchardt, G. *J. Chem. Thermodyn.* **1984**, *16*, 1103.
- (92) Schaefer, G. W.; Van Zyl, A.; Weppner, W. *Solid State Ionics* **1990**, *40/41*, 154.
- (93) Yamaguchi, S.; Iguchi, Y.; Imai, A. *Solid State Ionics* **1990**, *40/41*, 87.
- (94) Yamaguchi, S.; Kimura, K.; Tange, M.; Iguchi, Y.; Imai, A. *Solid State Ionics* **1988**, *26*, 183.
- (95) Rög, G.; Kozifski, S. *J. Chem. Thermodyn.* **1983**, *15*, 111.
- (96) Rög, G.; Kozifski, S.; Kozłowska-Rög, A. *Electrochim. Acta* **1981**, *26*, 1819.
- (97) Hong, H. Y.-P. *Mater. Res. Bull.* **1976**, *11*, 173.
- (98) Goodenough, J. B.; Hong, H. Y.-P.; Kafalas, J. A. *Mater. Res. Bull.* **1976**, *11*, 203.
- (99) Nomura, K.; Ikeda, S.; Ito, K.; Einaga, H. *Bull. Chem. Soc. Jpn.* **1992**, *65*, 3221.
- (100) Nomura, K.; Ikeda, S.; Ito, K.; Einaga, H. *J. Electroanal. Chem.* **1992**, *326*, 351.
- (101) Nomura, K.; Ikeda, S.; Masuda, H.; Einaga, H. *Chem. Lett.* **1993**, 893.
- (102) Christidis, P. C.; Rentzeperis, P. J. *Z. Kristallogr.* **1975**, *141*, 233.
- (103) Kohler, H.; Schulz, H. *Mater. Res. Bull.* **1985**, *20*, 1461.
- (104) Kohler, H.; Schulz, H. *Mater. Res. Bull.* **1986**, *21*, 23.
- (105) Ikeda, S.; Nomura, K.; Ito, K.; Einaga, H. *Solid State Ionics* **1994**, *70/71*, 153.
- (106) Ikeda, S.; Takahashi, M.; Ishikawa, J.; Ito, K. *Solid State Ionics* **1987**, *23*, 125.
- (107) Ikeda, S.; Kanbayashi, Y.; Nomura, K.; Kasai, A.; Ito, K. *Solid State Ionics* **1990**, *40/41*, 79.
- (108) Nomura, K.; Ikeda, S.; Ito, K.; Einaga, H. *Chem. Lett.* **1992**, 1897.
- (109) Alami Talbi, M.; Brochu, R.; Parent, C.; Rabardel, L.; Le Flem, G. *J. Solid State Chem.* **1994**, *110*, 350.
- (110) Esaka, T.; Kobayashi, Y.; Obata, H.; Iwahara, H. *Solid State Ionics* **1989**, *34*, 287.
- (111) Byström, A.; Byström, A. M. *Acta Crystallogr.* **1950**, *3*, 146.
- (112) Byström, A.; Byström, A. M. *Acta Crystallogr.* **1951**, *4*, 469.
- (113) Bursill, L. A.; Grzanic, G. *Acta Crystallogr. B* **1980**, *36*, 2902.
- (114) Iwauchi, K.; Ikeda, Y. *Phys. Stat. Sol. A* **1992**, *130*, 449.
- (115) Onoda, Y.; Watanabe, M.; Fujiki, Y.; Kudo, Y.; Erata, T.; Yoshikado, S.; Ohachi, T.; Taniguchi, I. *Solid State Ionics* **1988**, *28-30*, 179.
- (116) Köhler, J.; Urland, W. *Z. Anorg. Allg. Chem.* **1997**, *623*, 231.
- (117) Köhler, J.; Urland, W. *Z. Anorg. Allg. Chem.* **1996**, *622*, 191.
- (118) Köhler, J.; Urland, W. *J. Solid State Chem.* **1996**, *127*, 161.
- (119) Köhler, J.; Urland, W. *Solid State Ionics* **1996**, *86/88*, 93.
- (120) Farrington, G. C.; Dunn, B.; Thomas, J. O. *Appl. Phys. A* **1983**, *32*, 159.
- (121) The following statement has been made by the authors concerning conductivity data which have been obtained from a "completely" ion exchanged  $Gd^{3+}$ - $\beta''$ - $Al_2O_3$  crystal with the composition  $Gd_{0.56}Mg_{0.67}Al_{10.33}O_{17}$ : "It is not clear what fraction of this conductivity is the result of  $Gd^{3+}$  ion motion compared to that of residual sodium ions." <sup>120</sup> See also ref 47.
- (122) Tietz, F.; Urland, W. *Key Eng. Mater.* **1991**, *59/60*, 175.
- (123) Tietz, F.; Urland, W. *Solid State Ionics* **1995**, *78*, 35.
- (124) Carrillo-Cabrera, W.; Thomas, J. O.; Farrington, G. C. *Solid State Ionics* **1983**, *9/10*, 245.
- (125) Köhler, J.; Urland, W. *Angew. Chem.* **1997**, *109*, 150; *Angew. Chem., Int. Ed. Engl.* **1997**, *36*, 85.
- (126) Köhler, J., PhD Thesis, University of Hannover/Germany, 1996.
- (127) Tietz, F.; Urland, W. *J. Alloys Compd.* **1993**, *192*, 78.
- (128) Tietz, F.; Urland, W. *Solid State Ionics* **1991**, *46*, 331.
- (129) Tietz, F.; Urland, W. *J. Solid State Chem.* **1992**, *100*, 255.
- (130) Kumar, R. V. *J. Alloys Compd.* **1997**, *250*, 501.
- (131) Jin, C.; Li, L.; Hong, Y. Ext. Abs. 11th Int. Conf. *Solid State Ionics* **1997**, 335.
- (132) Foster, L. M.; Arbach, G. V. *J. Electrochem. Soc.* **1977**, *124*, 164.
- (133) Foster, L. M.; Stumpf, H. C. *J. Am. Chem. Soc.* **1973**, *73*, 1590.
- (134) Rohrer, G. S.; Thomas, J. O.; Farrington, G. C. *Chem. Mater.* **1991**, *3*, 325.
- (135) Kahn-Harari, A.; Aka, G.; Théry, J. *J. Solid State Chem.* **1991**, *91*, 71.
- (136) Aka, G.; Théry, J.; Vivien, D. *Solid State Ionics* **1990**, *39*, 225.
- (137) Aka, G.; Kahn-Harari, A.; Lucas, V.; Théry, J.; Vivien, D. *Solid State Ionics* (Proc. Symp. A2, Int. Conf. Adv. Mater.) **1992**, 271.
- (138) Shannon, R. D. *Acta Crystallogr. A* **1976**, *32*, 751.
- (139) Wang, X. E.; Lejus, A. M.; Vivien, D.; Collongues, R. *Mater. Res. Bull.* **1988**, *23*, 43.
- (140) Sun, W. Y.; Yen, T. S.; Tien, T. Y. *J. Solid State Chem.* **1991**, *95*, 424.
- (141) Kahn, A.; Lejus, A. M.; Madsac, M.; Théry, J.; Vivien, D.; Bernier, J. C. *J. Appl. Phys.* **1981**, *52*, 6864.
- (142) Warner, T. E.; Fray, D. J.; Davies, A. *Solid State Ionics* **1996**, *92*, 99.
- (143) Warner, T. E.; Fray, D. J.; Davies, A. *J. Mater. Sci.* **1997**, *32*, 279.
- (144) Dyer, A. J.; White, E. A. D. *Trans. Br. Ceram. Soc.* **1964**, *63*, 301.
- (145) Iyer, P. N.; Smith, A. J. *Acta Crystallogr.* **1967**, *23*, 470.
- (146) George, A. M.; Virkar, A. N. *J. Phys. Chem. Solids* **1988**, *49*, 743.
- (147) Nassau, K.; Levinstein, H. J.; Loiacono, G. M. *J. Phys. Chem. Solids* **1965**, *26*, 1805.
- (148) Abrahams, S. C.; Bernstein, J. L. *J. Chem. Phys.* **1966**, *45*, 2745.
- (149) Borchardt, H. J. *J. Chem. Phys.* **1963**, *39*, 504.
- (150) Bykov, A. B.; Chipkin, A. P.; Demyanets, L. N.; Doromin, S. N.; Genkina, E. A.; Ivanov-Shits, A. K.; Kondratyuk, I. P.; Makosomov, B. A.; Melnikov, O. K.; Muradyan, L. N.; Simonov, V. I.; Timofeeva, V. A. *Solid State Ionics* **1990**, *38*, 31.
- (151) Verma, B. K.; Lal, H. B. *Mater. Res. Bull.* **1981**, *16*, 1579.
- (152) Pratrapp, V.; Gaur, K.; Lal, H. B. *Mater. Res. Bull.* **1987**, *22*, 1381.
- (153) Kobayashi, Y. PhD Thesis, Osaka University/Japan, 1998.
- (154) Imanaka, N.; Kobayashi, Y.; Adachi, G. *Chem. Lett.* **1995**, 433.
- (155) Imanaka, N.; Adachi, G. *J. Alloys Comput.* **1997**, *250*, 492.
- (156) Köhler, J.; Kobayashi, Y.; Imanaka, N.; Adachi, G. *Solid State Ionics* (Ext. Abs. 11th Int. Conf.) **1997**, *340*; *Solid State Ionics*, in press.
- (157) Imanaka, N.; Kobayashi, Y.; Tamura, S.; Adachi, G. *Solid State Ionics* (Ext. Abs. 11th Int. Conf.) **1997**, *337*; *Solid State Ionics*, submitted for publication.